Deep-Learning for Epicardial Adipose Tissue Assessment with Computed Tomography: Implications for Cardiovascular Risk Prediction

Deep-Learning for Epicardial Adipose Tissue Assessment with Computed Tomography: Implications for Cardiovascular Risk Prediction

Henry W. West BMedSci (Hon1), MBBS[a,b], Muhammad Siddique PhD[a,b,c], Michelle C. Williams MD PhD[d], Lucrezia Volpe BSc[a,b], Ria Desai BSc[e], Maria Lyasheva MPhil[a,b], Sheena Thomas BSc[a,b], Katerina Dangas BSc [a,b], Christos P Kotanidis MD[a], Pete Tomlins PhD[a,c], Ciara Mahon MD[f], Attila Kardos MD PhD[g,h], David Adlam MD PhD[i], John Graby MD[j], Jonathan C.L. Rodrigues MD PhD[j], Cheerag Shirodaria MD MBA[c,k], John Deanfield MD PhD[l], Nehal N. Mehta MD[m], Stefan Neubauer MD PhD[b], Keith M. Channon MD PhD[a,b], Milind Y. Desai MD MBA[n], Edward D. Nicol MD MBA[f,o], David E. Newby MD PhD[d], Charalambos Antoniades MD PhD[a,b]*, on behalf of the ORFAN Investigators

[a]Acute Multidisciplinary Imaging and Interventional Centre, Radcliffe Department of Medicine, University of Oxford, Oxford, England, UK

[b]Division of Cardiovascular Medicine, Radcliffe Department of Medicine, University of Oxford, Oxford, England, UK

[c]Caristo Diagnostics Pty Ltd, Oxford, England, UK

[d]Centre for Cardiovascular Science, University of Edinburgh, Edinburgh, Scotland, UK

[e]Northwestern University, Evanston, IL, USA

[f]Royal Brompton and Harefield NHS Foundation Trust, London, England, UK

[g]Translational Cardiovascular Research Group, Department of Cardiology, Milton Keynes University Hospital, Milton Keynes, England, UK

[h]Faculty of Medicine and Health Sciences, University of Buckingham, Buckingham, England, United Kingdom,

[i]Department of Cardiovascular Sciences and NIHR Leicester Biomedical Research Centre, University of Leicester, Leicester, England, UK

[j]Royal United Hospitals Bath NHS Foundation Trust & Department of Health, University of Bath, Bath, England, UK

[k]Department of Cardiology, Oxford University Hospitals NHS Foundation Trust, Oxford, England, UK

[l]University College London, London, England, UK

[m]National Heart, Lung, and Blood Institute, National Institutes of Health, Bethesda, MD, USA

[n]The Cleveland Clinic, Cleveland, OH, USA

[o]School of Biomedical Engineering and Imaging Sciences, King's College London, London, England, UK

Running title: Automatic EAT assessment for risk prediction

***Address for Correspondence:**

Prof Charalambos Antoniades MD PhD FRCP FESC

British Heart Foundation Chair of Cardiovascular Medicine

Acute Multidisciplinary Imaging & Interventional Centre, University of Oxford

John Radcliffe Hospital, Oxford OX3 9DU, United Kingdom,

Tel: +44-1865-228340, Fax: +44-1865-740352

e-mail: charalambos.antoniades@cardiov.ox.ac.uk

Twitter: Corresponding author @Charis_Oxford First author @henrywwest

Financial Disclosures: This study received support from the British Heart Foundation (TG/19/2/34831) and the EU Commission Horizon 2020 program via the MAESTRIA Consortium (965286). CA acknowledges support from the British Heart Foundation (CH/F/21/90009, TG/19/2/34831 and RG/F/21/110040), Innovate UK grant 104472 and the National Consortium of Intelligent Medical Imaging (NCIMI) through the Industry Strategy Challenge Fund (Innovate UK Grant 104688). DA

acknowledges support from the Leicester NIHR Biomedical Research Centre. MCW is supported by the British Heart Foundation (FS/ICRF/20/26002)

Disclosures: CA, CS and KC are founders, shareholders and directors of Caristo Diagnostics Ltd., a CT-image analysis company. CS, PT and MS are employees of Caristo Diagnostics Ltd. DA has received research funding and in-kind support for unrelated research from Astra Zeneca Inc. He has received an educational grant from Abbott Vascular Inc to support a clinical research fellow for unrelated research. He has also conducted consultancy for GE Inc to support research funds for unrelated research. MCW serves on the speaker bureau for Canon Medical Systems. CA is also inventor of patent US10,695,023B2, PCT/GB2017/053262, GB2018/1818049.7, GR20180100490 and GR20180100510, licensed through exclusive license to Caristo Diagnostics. The remaining authors have nothing to disclose.

Acknowledgements: We thank all participants and patients in the research studies utilised in this study, including ORFAN, AdipoRedOx and the SCOT-HEART trial. We also thank all radiographers and technical staff who contributed to the inclusion of patients in these studies. We thank all ORFAN Study Investigators from all sites, listed in the Author Supplement. C.A. is the guarantor of this original article.

ABSTRACT *(250 words)*

BACKGROUND: Epicardial adipose tissue volume (EAT) is a marker of visceral obesity that can be measured in coronary CT angiograms (CCTA). The clinical value of integrating this measurement in routine CCTA interpretation has not been documented.

OBJECTIVE: To develop a deep-learning network (DLN) for automated quantification of EAT from CCTA, test it in technically challenging patients, and validate its prognostic value in routine clinical care.

METHODS: The DLN was trained and validated to auto-segment EAT in 3720 CCTA scans from the Oxford Risk Factors And Non-invasive imaging cohort. The model was tested in patients with challenging anatomy and scan artefacts and applied to a longitudinal cohort of 253 post-cardiac surgery patients and 1558 patients from the SCOT-HEART trial, to investigate its prognostic value.

RESULTS: External validation of the DLN yielded a concordance correlation coefficient of 0.970 for machine vs human. EAT was associated with coronary artery disease (OR[95%CI] per SD increase in EAT 1.13[1.04-1.30] p=0.01), and atrial fibrillation (AF) (1.25[1.08-1.40], p=0.03), after correction for risk factors (including BMI). EAT predicted all-cause mortality (HR[95%CI] per SD = 1.28[1.10-1.37], p=0.02), myocardial infarction (1.26[1.09-1.38] p=0.001) and stroke (1.20[1.09-1.38] p=0.02) independently of risk factors in SCOT-HEART (5y follow-up). It also predicted in-hospital (HR[95%CI] = 2.67[1.26-3.73], p=< 0.01) and long-term post-cardiac surgery AF (7y follow-up; HR[95%CI] = 2.14[1.19-2.97], p=< 0.01).

CONCLUSIONS: Automated assessment of EAT is possible in CCTA, including in challenging patients; it forms a powerful marker of metabolically unhealthy visceral obesity, which could be used for cardiovascular risk stratification.

KEY WORDS: Computed tomography, deep-learning, adipose tissue, visceral fat, atherosclerosis, atrial fibrillation

ABBREVIATION LIST

BMI	Body mass index
BSA	Body surface area
CAC	Coronary artery calcium
CAD	Coronary artery disease
CCC	Lin's concordance correlation coefficient
CCTA	Coronary computed tomography angiography
DLN	Deep-learning network
EAT	Epicardial adipose tissue
HU	Hounsfield Units
MI	Myocardial infarction
ORFAN	The Oxford Risk Factors And Non Invasive Imaging Study
ROC	Receiver operator characteristic

INTRODUCTION

Coronary computed tomography angiography (CCTA) is used to evaluate coronary artery disease (CAD) risk(1), with guidelines in Europe(2) and USA(3) recommending CCTA for assessment of patients with chest pain. The use of CCTA for detecting CAD is increasing world-wide and it is likely that further valuable information within CCTA scans that is currently not fully utilised in clinical practice could improve risk assessment and patient management for cardio-metabolic diseases, with multiple such technologies being discovered through the uptake of artificial intelligence methods in research and practice(4).

Adipose tissue is recognised as a key regulator of cardiovascular health and disease, exerting both protective and deleterious effects on the cardiovascular system(5). Epicardial adipose tissue (EAT) is a metabolically active depot of visceral fat(5), and may be a feature of metabolically unhealthy obesity and the metabolic syndrome (6). Indeed, EAT volume has been associated with multiple distinct cardiovascular diseases including CAD and atrial fibrillation (AF)(7). The EAT volume is generally considered to be a marker of visceral obesity, as opposed to more sophisticated metrics such as the peri-coronary Fat Attenuation Index, which specifically captures the degree of coronary inflammation, and has prognostic value over and above that of EAT volume(8). CCTA provides the non-invasive gold standard measurement of EAT volume due to its excellent spatial resolution. However, manual quantification is laborious and currently falls outside the scope of routine CCTA interpretation. If clinical utility of automated EAT volume quantification could be demonstrated and found to be feasible in technically challenging CCTA patients, it is possible that this measure could become part of standard of care.

In this study we developed and validated a DLN for the automated quantification of EAT volume, which was then tested in real-world CCTA patients with commonly encountered image quality issues to ensure validity. Then, we applied the fully automated EAT quantification tool to investigate the

clinical association of EAT volume with relevant cross-sectional and longitudinal disease outcomes (Central illustration).

METHODS

Study populations

Each study (Oxford Risk Factors And Non Invasive Imaging Study (ORFAN), AdipoRedOx and the Scottish COmputed Tomography of the HEART (SCOT-HEART) trial) received ethical approval. The full ethics, population descriptions, variable definitions, laboratory techniques, and CCTA acquisition and retrieval protocols are outlined in the Supplementary Methods. Briefly, The ORFAN Study (NCT05169333) is an international multi-centre prospective cohort study which collects CCTA scans and patient clinical data from those who are undergoing or have undergone CCTA since 2005 (www.oxhvf.com/the-orfan-study). For this analysis, data was utilised from across four NHS sites in England and one in the USA (Figure 1). The AdipoRedOx study involves patients who are undergoing cardiac surgery; as part of the study patients undergo CCTA shortly after their operation and are prospectively followed-up for clinical outcomes via NHS Digital (see Supplement). The SCOT-HEART trial included clinical patients with suspected angina due to coronary heart disease, who were followed up for 5 years post-CCTA for clinical outcomes (see Supplement).

Overall study design

The overall approach to the development of the DLN, the internal and external validation, and the application of the DLN in external cohorts for ascertainment of clinical utility is outlined in Figure 2. In summary, 2200 CCTA scans from the ORFAN Study were utilised for training the DLN for the detection of the whole heart within the bounds of the pericardium. Following training, an initial assessment of model performance was performed in 100 unseen ORFAN Study scans (see Supplementary Figure 1 and 2). Three separate groups of 200 unseen scans from the ORFAN Study were utilised for fine-tuning the model through three iterations of feedback learning.

The DLN was tested internally on 200 unseen ORFAN Study scans from the UK sites of the study. External validation was performed on 720 unseen scans from USA sites of the ORFAN Study. The DLN was then applied to unseen scans from challenging clinical populations test the model in patients with challenging anatomy and/or commonly occurring scan artefacts. Finally, the model was tested in unseen external scans of the SCOT-HEART trial for real world evaluation of the prognostic value of EAT volume as a marker of metabolically unhealthy obesity. The model was also applied within the AdipoRedOx Study to test the prognostic value of EAT volume on the risk of in-patient post-cardiac surgery AF (>30s AF on monitoring) and long-term AF (paroxysmal, persistent, or chronic) following surgery were investigated

Developing the DLN for automated segmentation and quantification of EAT volume

Manual segmentation of the 2200 CCTA and the iterations of scans for feedback learning of the DLN, and the automated extraction of EAT volume from the heart segmentation were performed using CaRi-Heart® version 2.2.1 (Caristo Diagnostics Ltd., Oxford, UK) (see Supplementary Figure 3)(9). A fully automated method for whole heart segmentation on CCTA scans was employed using a 3D Residual-U-Net neural network architecture for volumetric segmentation of CCTA (Supplementary Methods). The architecture of the DLN is demonstrated in Figure 3A.

Internal validation

A random sample of 200 sequestered CCTAs from the UK sites in the ORFAN study were utilised for internal validation of the DLN. Human segmentation of these scans was undertaken blind to all other data.

External validation

A sample of 720 unseen CCTA from the Cleveland Clinic, OH, USA, site of the ORFAN Study were utilised for external validation of the algorithm – as a broad external validation cohort(10). The manual segmentation of these scans was undertaken blind to all other data.

Statistical analysis

For inter-reader repeatability testing and human versus automated model assessment of testing data (preliminary testing, internal/external validation, and challenging clinical populations) agreement was assessed by using concordance correlation coefficients (CCC) with scatterplots and Bland-Altman analysis for significance of bias. When applied in a cohort-wide setting in the AdipoRedOx and SCOT-HEART studies, all EAT volumes were standardised by patient body surface area (BSA) using the Du Bois formula[22].

For cross-sectional analysis of disease risk conveyed by EAT volume, multiple-adjusted logistic regression was used for calculation of the odds-ratio of prevalent disease (AF at time of CCTA and obstructive CAD from CCTA) at the time of the CCTA given increase in EAT by one standard deviation (SD). All analysis were adjusted for a standard set of cardiovascular disease (CVD) risk factors that are listed within all figure legends. Longitudinal assessment of the prognostic value of EAT volume was performed by multivariable Cox regression models adjusted for the standard set of clinical risk factors for each outcome. Both odds ratios and hazard ratios are reported per one SD increase in EAT volume. Analysis of all SCOT-HEART trial risk models was repeated with the inclusion of only variables in each model that were found to have a statistically meaningful association with the relevant outcome (dependent variable) in univariate analysis, at the level of $p \leq 0.1$ (see Supplementary Methods, & Supplementary Table 1). Supplementary analysis of AdipoRedOx Study risk models was performed with AF specific risk factors (see Supplementary Methods).

Receiver operator characteristic curves for the discrimination of obstructive CAD from CCTA and MI were plotted with a CVD risk factor models vs traditional risk factor model plus the addition of EAT volume. Area under the curve analysis was undertaken to compare the models for each outcome.

We selected the optimum unified cut-off for EAT volume prognostication for all-cause mortality, fatal/non-fatal MI and fatal/non-fatal stroke in SCOT-HEART by identifying the value that maximised Youden's J statistic (sum of sensitivity and specificity) on time-dependent ROC curve analysis for all-cause mortality, fatal/non-fatal MI and fatal/non-fatal stroke to ensure an optimum balance between

sensitivity and specificity in our models. For consistency, the same approach was utilised to select the optimum cut-off for EAT volume prognostication for in-hospital post-operative and long-term AF risk within the severe CAD population of the AdipoRedOx Study. Further statistical analysis is in the Supplementary Methods.

RESULTS

The geographic location, demographics, clinical risk factors, and CCTA scan technical parameters for all ORFAN Study cohorts utilised in DLN training, validation and external testing are shown in Table 1. The demographics and scan characteristics of the external clinical cohorts for which the DLN were applied following development are shown in Table 2. The relevant clinical outcomes for the prospective clinical cohorts are presented in Supplementary Table 2. In all cohorts where EAT volumes were quantified, both manually and automatically, the values were normally distributed.

Inter-reader repeatability for EAT segmentation and whole heart segmentation

The inter-observer variability between two expert analysts of the Oxford Academic Cardiovascular Computed Tomography Core Lab (OXACCT) core lab was evaluated in 100 randomly selected patients from the UK sites of ORFAN. CCC for EAT volume was excellent between readers at 0.970, and the bias was non-significant at mean[95% agreement] of 2.1[-3.9-6.1]cm^3, p= 0.74 (Supplementary Figure 5A-B). For the whole heart segmentation volume CCC was also excellent at 0.969 with non-significant bias of 15.2[-7.5-23.1]cm^3 p=0.08 (Supplementary Figure 5C-D).

Internal validation of the model

Final internal validation occurred following three iterations of feedback learning to enhance the performance of the model. The median[IQR] EAT volume in internal validation was 120.9[95.1-156cm^3]. When applied to 200 unseen scans from the UK sites of the ORFAN Study, the CCC was 0.972 (Figure 4A). The bias in Bland-Altman analysis (Figure 4B) was also non-significant at 6.1[-11.1-15.7]cm^3, p = 0.19.

External validation of the model

The final deep-learning model was applied to 720 unseen scans from the US sites of the ORFAN Study. The mean automated analysis time for the automated segmentation was 12.4 seconds compared to mean manual segmentation time of 18 minutes and 20 seconds. The median[IQR] EAT volume in external validation was 169.3[111.6-241.7]cm^3. The CCC for the automated deep-learning model versus human expert segmentation in the external validation cohort was excellent, at 0.970 (Figure 4C) and the bias in Bland-Altman analysis (Figure 4D) was non-significant at 3.2[-13.6-17.2]cm^3, p = 0.20.

Validation of the automated model for EAT volume quantification in challenging clinical populations

Excellent CCC for automated EAT segmentation versus human expert segmentation was achieved in all challenging patient groups: Patient's with recent cardiac surgery (<6 weeks post operation) CCC = 0.960 (Figure 5A – green); patients with BMI ≥ 40, CCC = 0.962 (Figure 5A – red); patients with reported CAC score of ≥ 400 (Figure 5B – green), CCC = 0.958; patients with significant metallic artefact within the pericardium, CCC = 0.955 (Figure 5B – red), and a combined patient group of recent open-heart surgery, BMI ≥ 30Kg/m^2 & CAC ≥ 400, CCC = 0.955 (Figure 5C).

Cross-sectional clinical correlations

At the time of the CCTA, application of the fully automated segmentation tool for quantification of EAT volume was found to be a significant independent predictor of the presence of AF at time of CCTA and obstructive CAD from CCTA (any one coronary vessel with ≥50% stenosis on CCTA), within 1,558 patients randomised to receive CCTA in the SCOT-HEART trial population.

When accounting for CVD risk factors the odds ratio (OR[95%CI]) of AF at time of CCTA per 1 standard deviation (SD) increase of EAT was 1.25[1.08-1.40] p=0.03 (Figure 6A). When accounting for CVD risk factors the OR of obstructive CAD from the CCTA per 1 SD increase of EAT was 1.13[1.04-1.30] p=0.01 (Figure 6B). Results with statistically selected risk factor adjustment is shown in Supplementary Figure 4.

Longitudinal EAT volume clinical correlations

Median follow up for the 1,558 patients randomised to receive CCTA in SCOT-HEART which were analysed was 4.8 years. There were 35 deaths of all causes (2.25%) of which 4 (0.25%) were deaths related with coronary heart disease. There were 8 fatal and non-fatal strokes (0.51%) and 39 fatal and non-fatal myocardial infarctions (2.5%).

The hazard ratio (HR[95%CI]) of all-cause mortality per 1 SD increase of EAT was 1.28[1.10-1.37] p=0.02, after accounting for CVD risk factors (Figure 6C). When adjusted for the same risk factors, the HR[95%CI] of non-cardiac mortality per 1 SD increase of EAT volume was 1.17[1.07-1.33] p=0.04 (Figure 6D). This constitutes a ΔHR of -0.10, confirming that EAT is a measure of visceral adipose tissue related with multiple fatal pathologies, unrelated to CAD. When accounting for CVD risk factors the HR of MI per 1 SD increase of EAT was 1.26[1.09-1.38] p=0.001 (Figure 6E). Finally, when accounting for the same risk factors, HR[95%CI] of stroke per 1 SD increase of EAT is 1.20[1.08-1.32] p=0.02 (Figure 6F). Results with statistically selected risk factor adjustment is shown in Supplementary Figure 4.

Adding EAT volume into a clinical model led to significant improvement in the ability to detect obstructive CAD on CCTA (any one coronary vessel with ≥50% stenosis on CCTA) cross sectionally (Figure 6G, ΔAUC 0.103 (p<0.01)) and improved the ability to predict future MI (both fatal and non-fatal) longitudinally (Figure 6H, ΔAUC 0.07 (P<0.01).

A single predictive value of EAT volume for long-term disease risk

To generate distinct clinical groups based around a single EAT volume cut-point, the SCOT-HEART trial population was dichotomised into high versus low EAT volume groups based on an optimum cut-off of 169.9cm^3 for the three primary outcomes of interest: all-cause mortality, fatal/non-fatal MI and fatal/non-fatal stroke. This cut-off was derived from a weighted Youden's J index analysis to generate a single value for application. Utilising this cut-point, there was significantly different adjusted hazard ratios for the low EAT group (<169.9cm^3) versus the high EAT group (≥169.9cm^3) for all outcomes. All analyses included multivariable adjustment for CVD risk factors including BMI.

High EAT volume values (≥169.9cm^3 vs <169.9cm^3) were associated with a higher prospective risk for both fatal and non-fatal myocardial infarction (adjusted HR 1.93[1.31-4.01] p<0·01; Figure 7A), both fatal and non-fatal stroke (2.25[1.07-4.72] p<0·01; Figure 7B), non-cardiac mortality (3.84[1.54-12.10] p<0·01; Figure 7C), and all-cause mortality (5.02[2.93-9.34] p<0·01; Figure 7D).

EAT volume and post-operative atrial fibrillation risk

Utilising 250 scans from patients in the AdipoRedOx Study, the longitudinal associations between EAT volume and in-patient post-operative AF (>30 seconds of AF on monitoring) and long-term AF (paroxysmal, persistent or chronic) following surgery were investigated.

Again, a weighted Youden's J index analysis was used to generate a single value to dichotomise the AdipoRedOx study population into high versus low EAT volume groups based on an optimum cut-off of 198.7cm^3 for the two primary outcomes of in-hospital post-operative AF and long-term post-operative AF. Utilising this cut-point, there was significantly different adjusted hazard ratios for the low EAT group (<198.7cm^3) versus the high EAT group (≥198.7cm^3) for both outcomes.

There were 97 events of in-hospital post-operative AF (38.8%) and 48 cases (19%) of new-onset AF in nation-wide NHS Digital data for the AdipoRedOx cohort. The Kaplan-Meier curve for in-hospital post-operative AF following cardiac surgery for high (≥198.7cm^3) EAT volume versus low (<198.7cm^3). High EAT volumes were associated with a significantly greater risk for in-patient post-operative AF following adjustment for CVD risk factors, with HR[95%CI] of 2.67[1.26-3.73] p<0.01, per 1 SD increase in EAT volume (Figure 8A). Equally, for long-term new-onset AF following cardiac surgery high risk EAT volumes were associated with a significantly greater risk for long-term AF, with HR[95%CI] of 2.14[1.19-2.97] p<0.01, per 1 SD increase in EAT volume (Figure 8B).

The addition of EAT volume into a CVD risk factor model significantly improved the prediction of new-onset in-hospital AF in ROC curve analysis (Figure 8C) with ΔAUC of +0.0.8 (p=0.03) for CVD risk factor model 1 with the addition of EAT volume, and ΔAUC of +0.11 (p<0.001) with the addition of the risk factor model plus EAT volume on top of CCTA derived LA volume alone. The same was

found for new-onset long-term AF (Figure 8D), with ΔAUC of +0.09 (p=0.04) for risk factor model 1 with the addition of EAT volume, and ΔAUC of +0.11 (p<0.001) over LA volume alone.

Identical analysis with adjustment for a selection of AF specific risk factors, including LA volume and NT-proBNP, is presented as Supplementary Figure 6, with EAT volume retaining significance in all models. There was no significant change in results for all post-operative AF risk analysis when BMI was replaced with waist-hip ratio (Supplementary Figure 7).

DISCUSSION

In this study we developed a deep-learning model for automated segmentation and quantification of EAT from CCTA images. The model was then validated in multiple cohorts, including commonly occurring challenging populations where manual segmentation is extremely difficult due to artefacts with good performance. Then we applied this automated model to the SCOT-HEART cohort, demonstrating a good prognostic value of EAT volume for all-cause mortality and cardiovascular events, as a possible measure of unhealthy visceral obesity relevant to cardiometabolic dysfunction, regardless of if EAT volume was used as a continuous variable or when used with a cut-off. Contrary to peri-coronary FAI, that captures the degree of coronary artery inflammation, and is predictive of cardiac (but not of non-cardiac) mortality, we now demonstrate that EAT volume is predictive of non-cardiac mortality, confirming its role as a broader biomarker of visceral obesity, that affects survival in a broader sense. We also demonstrate that this measurement has important prognostic value for post-operative AF in patients undergoing cardiac surgery, beyond known post-operative risk models including LA volume and NT-proBNP. Fully automated measurement of EAT volume incorporated into routine interpretation of CCTA promises to significantly improve the risk stratification of patients, across several important clinical outcomes.

We developed a deep-learning model utilising a single network for the fully automated and rapid quantification of EAT volume from CCTA. Previous automated models for EAT quantification have predominately been in small cohorts (11,12). Most relevant is Commandeur et al(13) who developed a

CNN capable of automated EAT segmentation and tested in the EISNER cohort, however no head-to-head comparison is made in this study. The model developed here achieves accurate EAT volume quantification in technically challenging yet commonly occurring clinical populations. The need for any AI-based radiology approaches to be applicable for all-comers is fundamental to patient acceptance and the future uptake of such technology. The DLN reduced EAT quantification time from an average of 18minutes when performed manually, to an average of 12seconds, rendering this tool usable in the clinical environment without adding workload to clinical teams.

EAT volume has previously been found to be associated with CVD metrics and outcomes including the presence of atherosclerosis (14) as well as coronary calcification progression(15). EAT is a source of numerous pro-inflammatory mediators that circulate well beyond the microcirculation of the heart to exert paracrine and endocrine effects on the cardiovascular and endocrine systems(5). We found EAT volume to be a significant predictor of all-cause mortality even with the exclusion of cardiac deaths. This suggests that the EAT may play a clinically significant role in broader metabolic diseases beyond atherosclerotic CAD. We propose that EAT volume should be treated as the gold standard for the detection of metabolically unhealthy visceral obesity and could form part of routine clinical interpretation of CCTA. This would shift the focus of CCTA examination as a purely structural assessment of the coronary arteries towards a more universal assessment of cardiovascular risk that considers a key visceral, metabolically sensitive, tissue depot.

EAT is in continuous bi-directional communication with the cardiovascular system(5). When there is discordance between adipose tissue and the cardiovascular system the former is thought to shift function and exerts detrimental effects on the vessels and the heart muscle(16), which may pre-dispose the patient to adverse outcomes such as those which we investigated. We found that EAT volume is predictive of non-fatal MI and stroke independent of BMI and following adjustment for other relevant disease risk factors.

We demonstrate that EAT volume is an independent predictor providing incremental value for post-operative AF regardless of patient BMI, LA volume, NT-pro-BNP, and other AF risk factors, indicating an important role for EAT in driving post-operative arrhythmogenesis. It is proposed that pro-inflammatory cytokines diffuse locally from dysfunctional EAT into the myocardium and contribute towards atrial myopathy(17), which drives the risk of AF.

Limitations of this study include that we did not have detailed adiposity data (e.g., waist-hip ratio), or mortality data available within the SCOT-HEART trial population to investigate the exact causes of non-cardiac mortality that could be driving our finding of elevated risk of all-cause mortality conveyed by EAT volume. There were only 4 cardiovascular deaths during the 5y follow-up in SCOT-HEART, limiting any cardiac mortality analysis. Other challenging clinical CCTA populations exist, such as those with congenital cardiac conditions, for which we lacked enough cases for testing of the deep-learning algorithm. Short-term AF risk data following cardiac surgery relied on inpatient monitoring only, without device monitoring following discharge.

Conclusions

We present a new deep-learning model that allows accurate, reproducible and rapid quantification of EAT volume on routine CCTA scans. We demonstrate that assessment of EAT volume can improve risk assessment for cardiovascular and non-cardiovascular outcomes independently of other risk factors including BMI. EAT volume is predictive of all-cause mortality and non-cardiac mortality, MI and stroke. EAT volume also conveys significant independent risk of post-cardiac surgery atrial fibrillation. Incorporating automated EAT volume quantification in CCTA reading protocols could improve global cardio-metabolic risk assessment and treatment planning for patients who undergo CCTA investigation, independently of the presence of coronary atherosclerosis.

CLINICAL PERSPECTIVE

Competency in Clinical Knowledge:

The automated quantification of epicardial adipose tissue (EAT) volume through an artificial intelligence approach on routine CT coronary angiography scans may allow improvements in disease risk assessment for cardiovascular event such as MI and stroke.

Translational Outlook:

The introduction of automated EAT assessment into standard CT coronary angiography interpretation could add significant value to patient care through enhanced prediction of disease risk for conditions such as coronary artery disease, stroke, and atrial fibrillation.

REFERENCES

1. Antoniades C, West HW. Coronary CT angiography as an 'one-stop shop' to detect the high-risk plaque and the vulnerable patient. European Heart Journal 2021;42:3853-3855.
2. Knuuti J, Wijns W, Saraste A et al. 2019 ESC Guidelines for the diagnosis and management of chronic coronary syndromes: The Task Force for the diagnosis and management of chronic coronary syndromes of the European Society of Cardiology (ESC). European Heart Journal 2019.
3. Gulati M, Levy PD, Mukherjee D et al. 2021 AHA/ACC/ASE/CHEST/SAEM/SCCT/SCMR Guideline for the Evaluation and Diagnosis of Chest Pain. 2021;78:e187-e285.
4. Oikonomou Evangelos K, West Henry W, Antoniades C. Cardiac Computed Tomography. Arteriosclerosis, Thrombosis, and Vascular Biology 2019;39:2207-2219.
5. Oikonomou EK, Antoniades C. The role of adipose tissue in cardiovascular health and disease. Nature Reviews Cardiology 2019;16:83-99.
6. Oikonomou EK, Siddique M, Antoniades C. Artificial intelligence in medical imaging: A radiomic guide to precision phenotyping of cardiovascular disease. Cardiovascular research 2020;116:2040-2054.
7. Nalliah CJ, Bell JR, Raaijmakers AJA et al. Epicardial Adipose Tissue Accumulation Confers Atrial Conduction Abnormality. J Am Coll Cardiol 2020;76:1197-1211.
8. Antonopoulos AS, Sanna F, Sabharwal N et al. Detecting human coronary inflammation by imaging perivascular fat. Sci Transl Med 2017;9.
9. Oikonomou EK, Antonopoulos AS, Schottlander D et al. Standardized measurement of coronary inflammation using cardiovascular computed tomography: integration in clinical care as a prognostic medical device. Cardiovascular research 2021;117:2677-2690.
10. van Smeden M, Heinze G, Van Calster B et al. Critical appraisal of artificial intelligence-based prediction models for cardiovascular disease European Heart Journal 2022;43:2921-2930.
11. Molnar D, Enqvist O, Ulén J et al. Artificial intelligence based automatic quantification of epicardial adipose tissue suitable for large scale population studies. Scientific Reports 2021;11:23905.

12. Spearman JV, Meinel FG, Schoepf UJ et al. Automated quantification of epicardial adipose tissue using CT angiography: evaluation of a prototype software. Eur Radiol 2014;24:519-26.

13. Commandeur F, Goeller M, Razipour A et al. Fully Automated CT Quantification of Epicardial Adipose Tissue by Deep Learning: A Multicenter Study. Radiology: Artificial Intelligence 2019;1:e190045.

14. Goeller M, Achenbach S, Marwan M et al. Epicardial adipose tissue density and volume are related to subclinical atherosclerosis, inflammation and major adverse cardiac events in asymptomatic subjects. Journal of cardiovascular computed tomography 2018;12:67-73.

15. Nakanishi R, Rajani R, Cheng VY et al. Increase in epicardial fat volume is associated with greater coronary artery calcification progression in subjects at intermediate risk by coronary calcium score: a serial study using non-contrast cardiac CT. Atherosclerosis 2011;218:363-8.

16. Antoniades C. 'Dysfunctional' adipose tissue in cardiovascular disease: a reprogrammable target or an innocent bystander? Cardiovascular research 2017;113:997-998.

17. Shen MJ, Arora R, Jalife J. Atrial Myopathy. JACC Basic Transl Sci 2019;4:640-654.

FIGURES & FIGURE LEGENDS

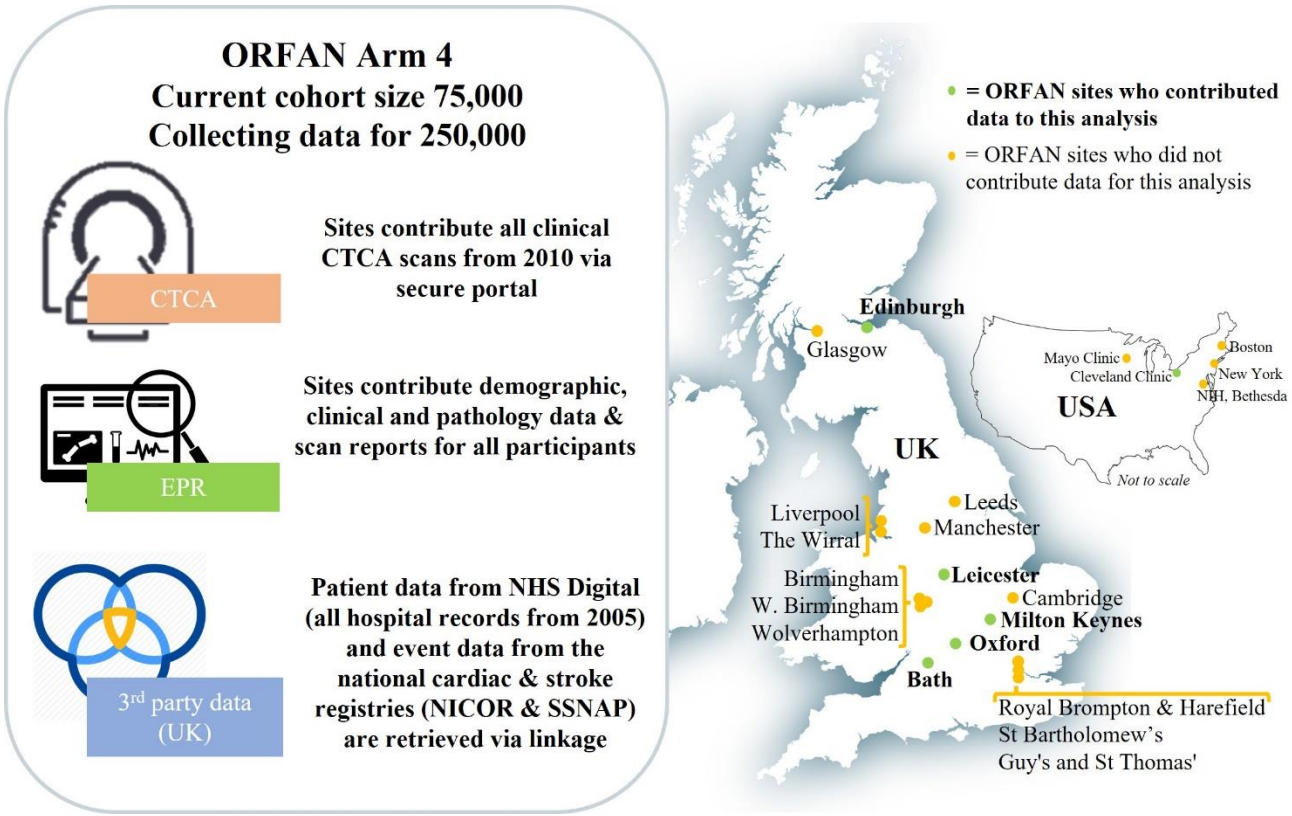

Figure 1. The ORFAN Arm 4 Study

The Oxford Risk Factors And Non Invasive Imaging Study (ORFAN) Arm 4 study is an international multi-centre retrospective cohort study of patients undergoing clinically indicated CCTA. The initial cohort size is 75,000 patients within the UK and 25,000 internationally, with ethically approved expansion underway for 250,000 patients. Within the UK, the study includes 17 NHS Trusts, with 4 contributing data for the current study. Data collected for each participant includes the CCTA scan, data from the local hospital electronic patient record (EPR) and data from authorised third parties, including NHS Digital (all hospital event data from 2005-now), NICOR (national cardiac event registry) and SSNAP (national stroke event registry).

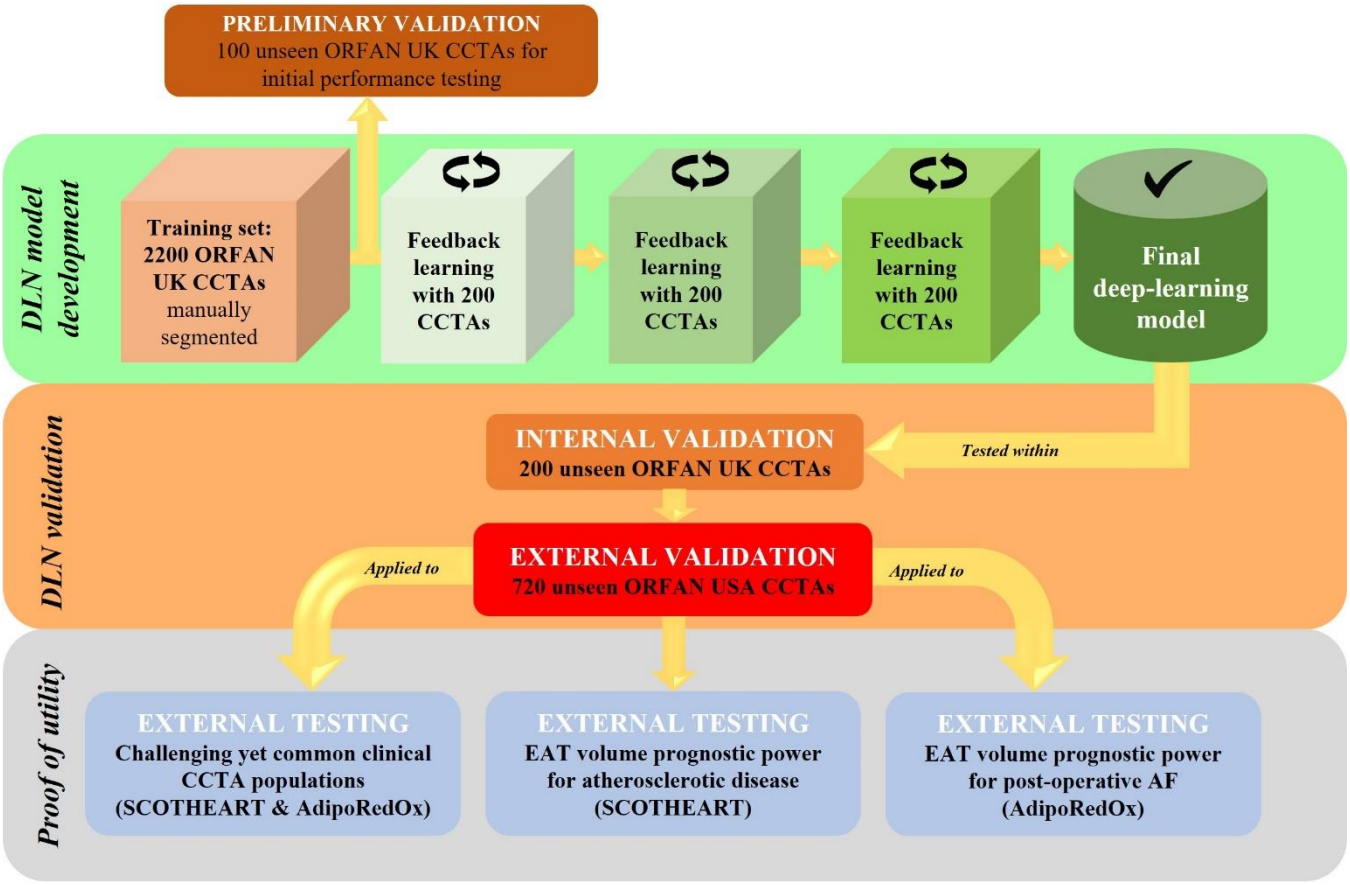

Figure 2. Study flow chart of model development, testing, and external application

Schematic representation of the scientific approach to the development of the deep-learning model, the validation of the model through internal and external cohorts, and the application of the automated EAT volume quantification tool to three groups of patients from the AdipoRedOx Study and SCOT-HEART trial.

CCTA: coronary computed tomography angiography; EAT: epicardial adipose tissue

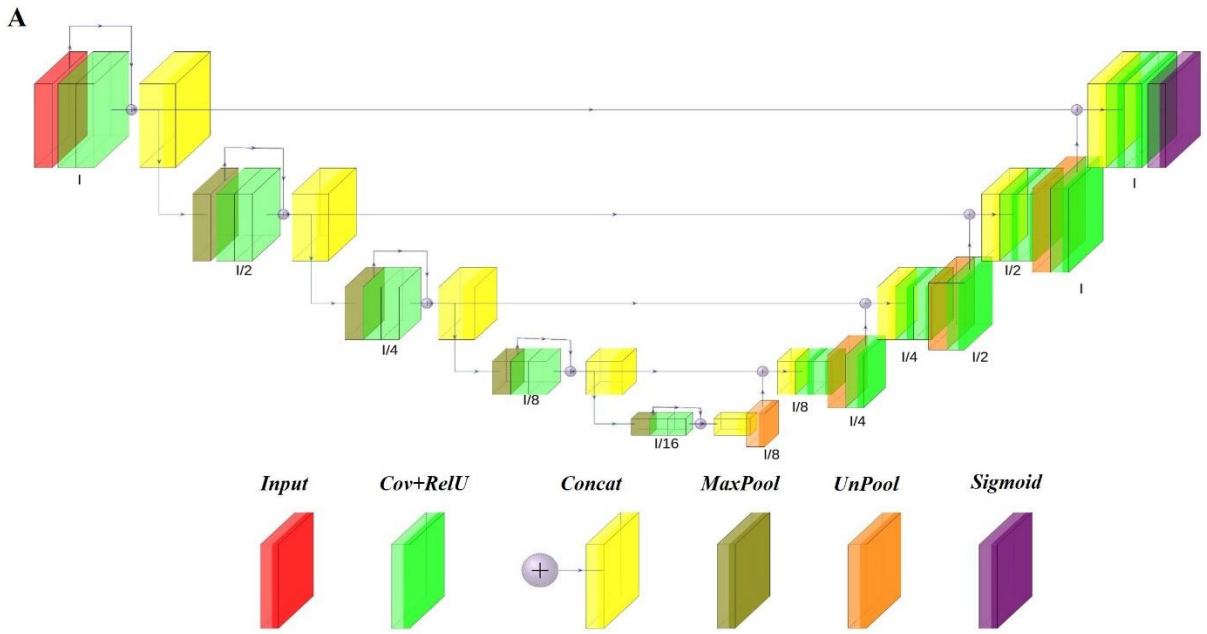
A
I
I/2
I/4
I/8
I/16
I/8
I/4
I/2
I
I/2
I
Input
Cov+RelU
Concat
MaxPool
UnPool
Sigmoid

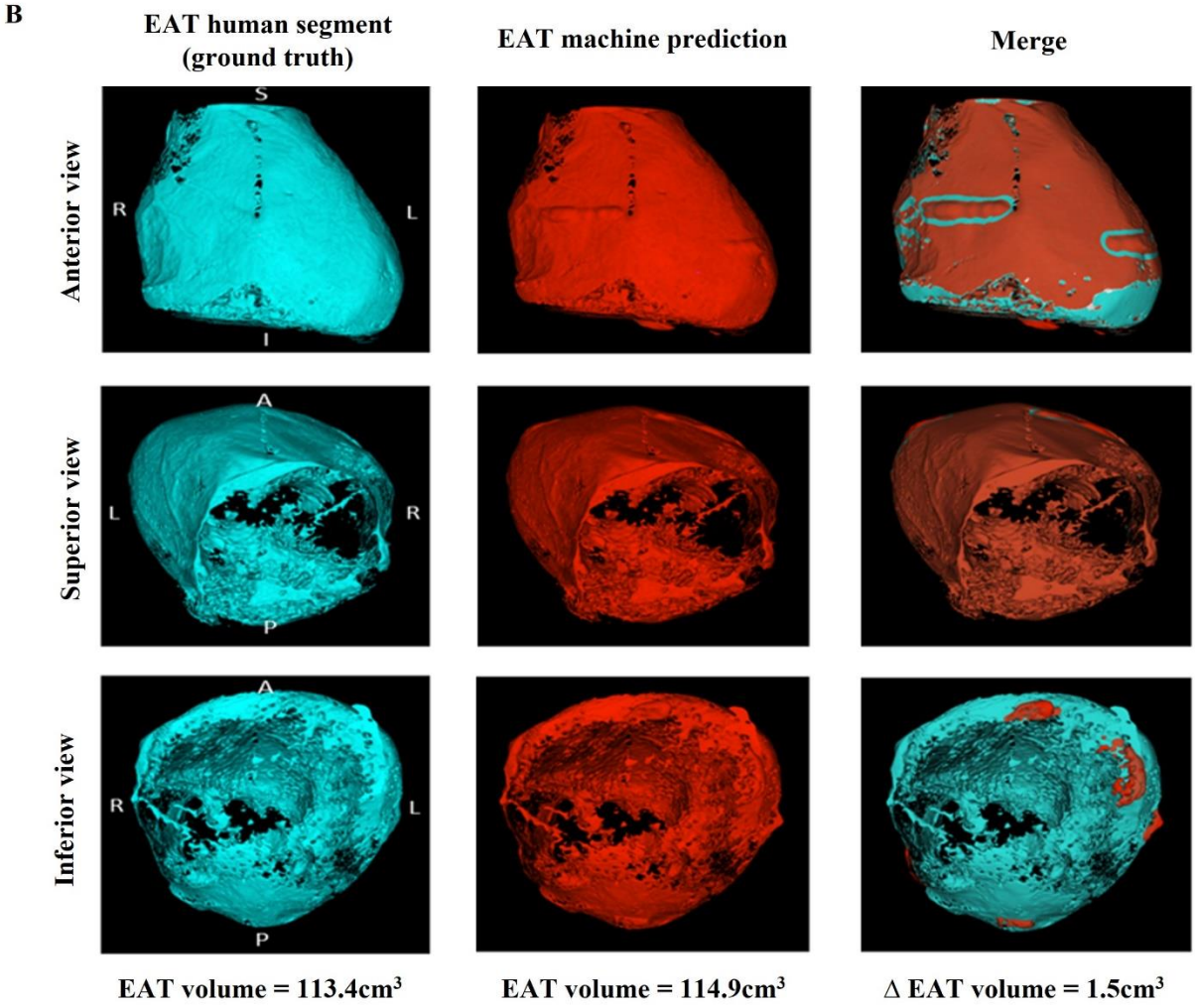
B
EAT human segment (ground truth)
EAT machine prediction
Merge
Anterior view
Superior view
Inferior view
S
R
L
I
A
L
R
P
A
R
L
P
EAT volume = 113.4cm³
EAT volume = 114.9cm³
Δ EAT volume = 1.5cm³

Figure 3. Schematic of the deep-learning model for automated segmentation of the whole heart within the pericardium (A), and example automated segmentation (B)

(A) Block diagram of the Residual U-Net based CNN architecture.

Details of each layer are provided in the Supplementary Methods.

(B) A single CCTA from the ORFAN study demonstrating human expert segmentation as ground truth, automated machine segmentation and a merge.

EAT: Epicardial adipose tissue; CCTA: coronary computed tomography angiography; I: inferior; L: left; R: right; S: superior.

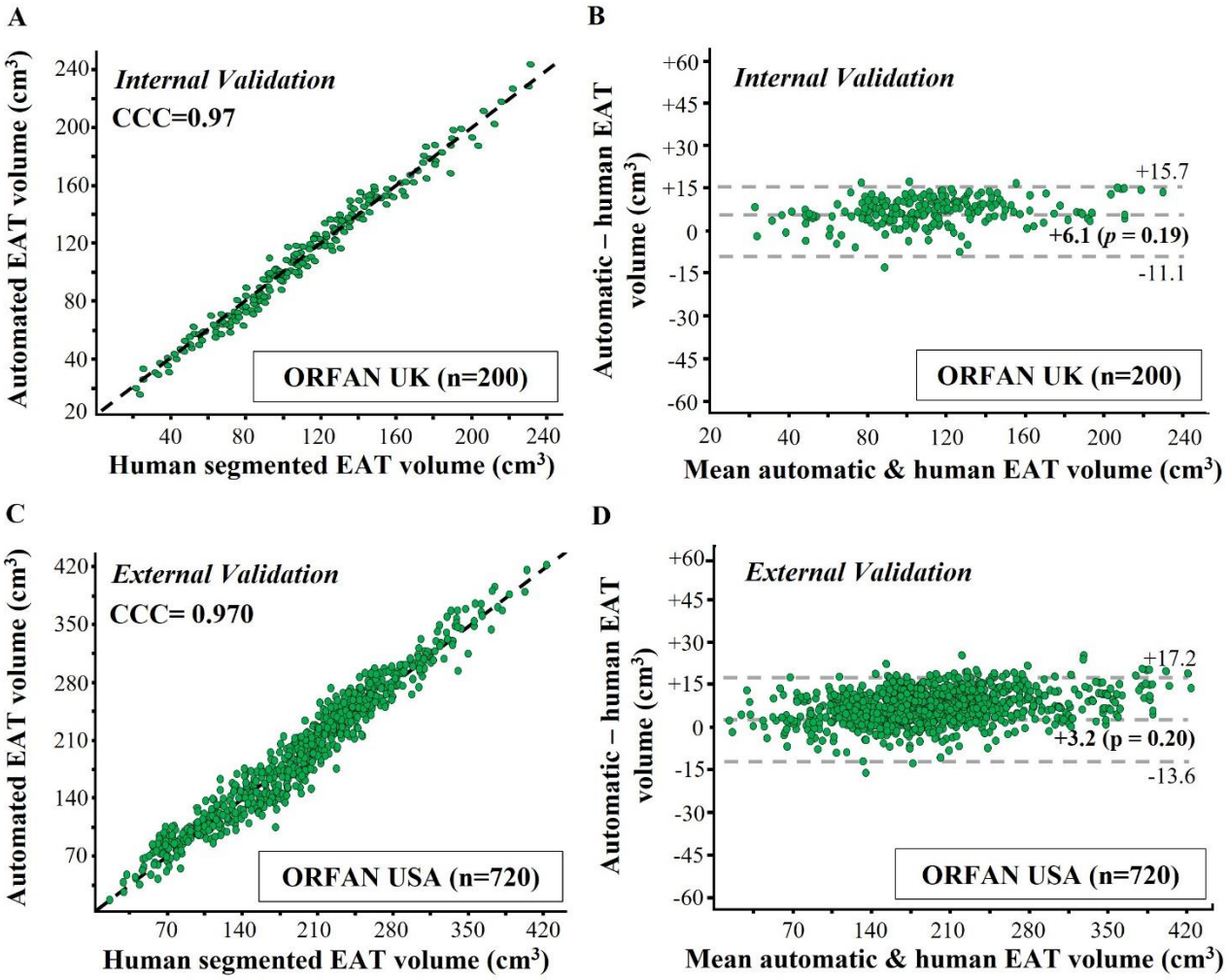

Figure 4. Validation of the deep-learning model

Following all training and fine-tuning of the algorithm, internal validation in 200 ORFAN UK cases occurred and is demonstrated in the scatterplot (A) and Bland-Altman plot (B). External validation in 720 ORFAN USA scans is shown in the scatterplot (C) and Bland-Altman plot (D). CCC: concordance correlation coefficient; EAT: epicardial adipose tissue

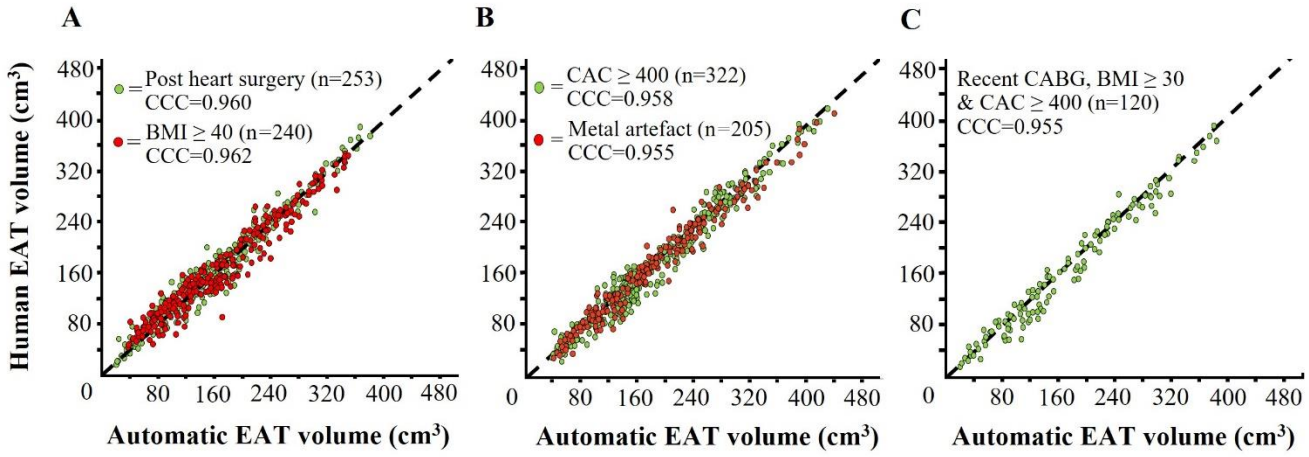

Figure 5. Validation of the automated deep-learning model in challenging clinical populations

The automated EAT volume quantification tool was applied to groupings of unseen CCTA from the AdipoRedox Study and the SCOT-HEART trial. (A) patients who underwent open heart surgery (CABG) up to 6 weeks prior to CCTA (green) and patients with BMI ≥ 40 (red); (B) patients with CAC ≥ 400 (green) and patients with significant metallic artefact within the pericardium (red); (C) patients who underwent open heart surgery (CABG) up to 6 weeks prior to the CCTA, had BMI ≥30 and CAC ≥400.

BMI: body mass index; CABG: coronary artery bypass graft surgery; CAC: coronary artery calcium score; CCC: concordance correlation coefficient; CCTA: coronary computed tomography angiography; EAT: epicardial adipose tissue.

Cross-sectional evaluation of EAT volume SCOT-HEART

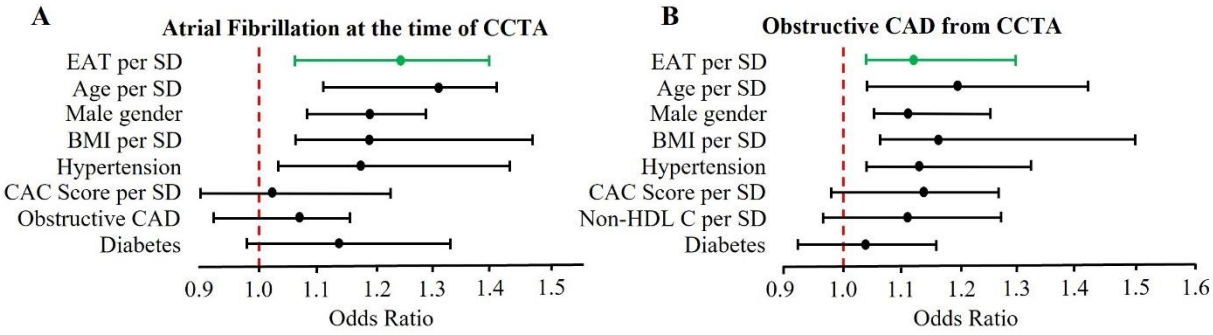

Longitudinal EAT volume and mortality in SCOT-HEART

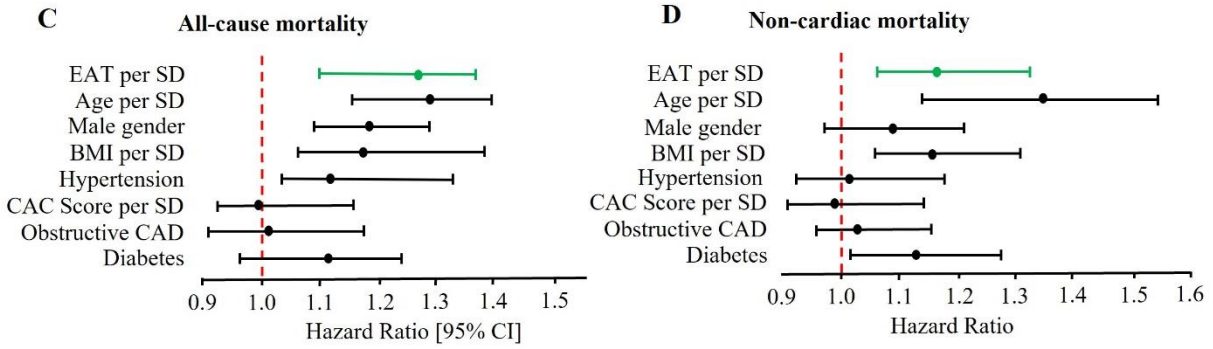

Longitudinal EAT volume and acute vascular events in SCOT-HEART

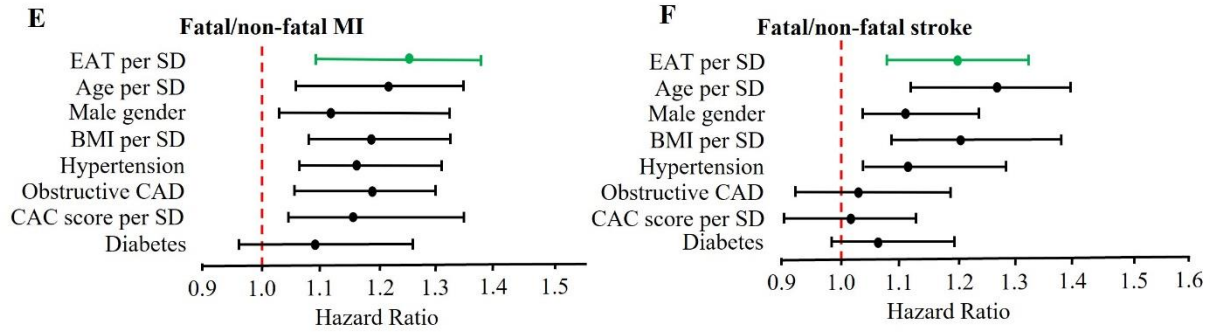

ROC curve analysis with EAT volume from SCOT-HEART

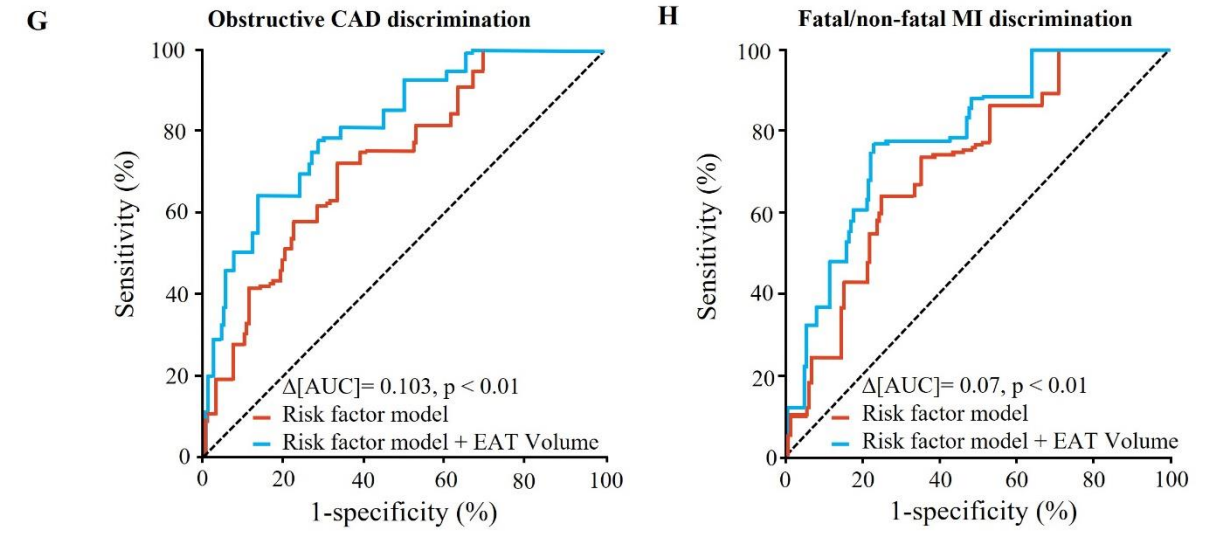

Figure 6. Cross-sectional and longitudinal associations between EAT volume and clinical outcomes in the SCOT-HEART trial

Plots of cross-sectional adjusted risk models for AF at the time of the scan, adjusted for age, gender, BMI, hypertension, CAC score, diabetes, and obstructive CAD as detected on CT (A); and obstructive CAD (any one coronary vessel with ≥50% stenosis on CCTA), adjusted for the same risk factors plus non-HDL-cholesterol and without obstructive CAD (B). Odds ratio is shown per 1 standard deviation (SD) increase in EAT volume for 1558 patients randomised to receive CCTA in the SCOT-HEART trial. Plots of longitudinal hazard ratios per 1 SD increase in EAT volume in 1558 patients randomised to receive CCTA in the SCOT-HEART trial are shown for all-cause mortality (C), and non-cardiac mortality (D), both with the same adjustment as for (A). Myocardial infarction (both fatal and non-fatal) (E) and stroke (both fatal and non-fatal) (F) are shown with the same adjustment. ROC curves are shown for the discrimination of obstructive CAD at the time of the CCTA (G) and longitudinal myocardial infarction (H). The risk factor model (blue) for each curve includes age, male gender, BMI, hypertension, non-HDL cholesterol, diabetes and CAC score, with obstructive CAD also included in the myocardial infarction model. Red in both curve is the risk factor model with the addition of EAT volume.

AF: atrial fibrillation; BMI: body mass index; CAC: coronary artery calcium score; EAT: epicardial adipose tissue; Non-HDL C.: non-high density lipoprotein cholesterol. *Continuous variables per 1-standard deviation increase; † = $P<0.05$

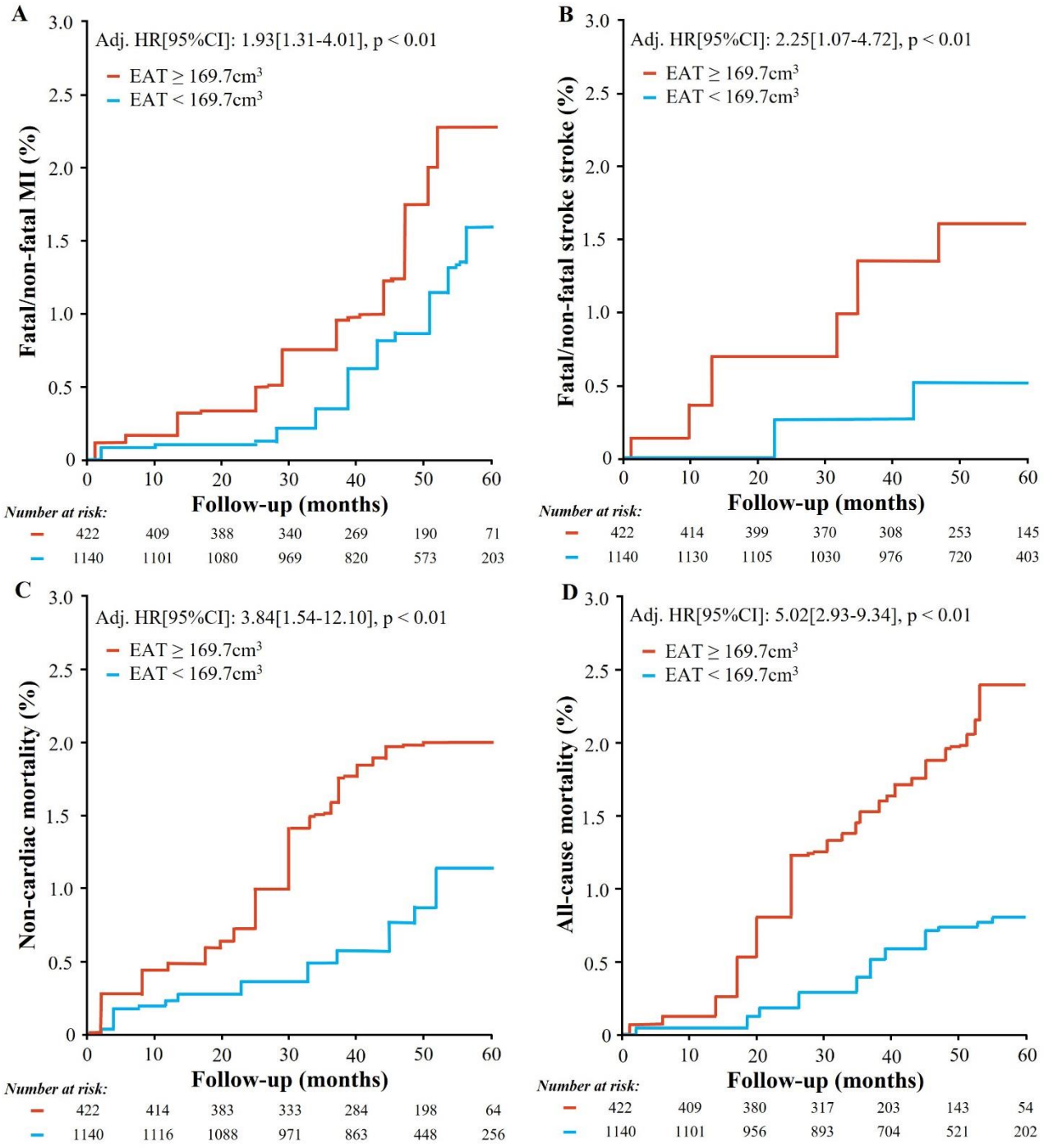

Figure 7. High EAT volume increases risk of major adverse events when assessed with a single cut-point

Utilising a single cut-point for high-risk patients in SCOT-HEART (high risk = EAT ≥169.9cm^3), Kaplan-Meier curves for (A) fatal/non-fatal myocardial infarction, (B) fatal/non-fatal stroke, (C) non-cardiac mortality, and (D) all-cause mortality, are demonstrated. All HR are adjusted for

age, sex, BMI, hypertension, diabetes mellitus, coronary artery calcium score (log-transformed) and obstructive CAD as derived from CCTA.

CI: confidence interval; EAT: epicardial adipose tissue; HR: hazard ratio

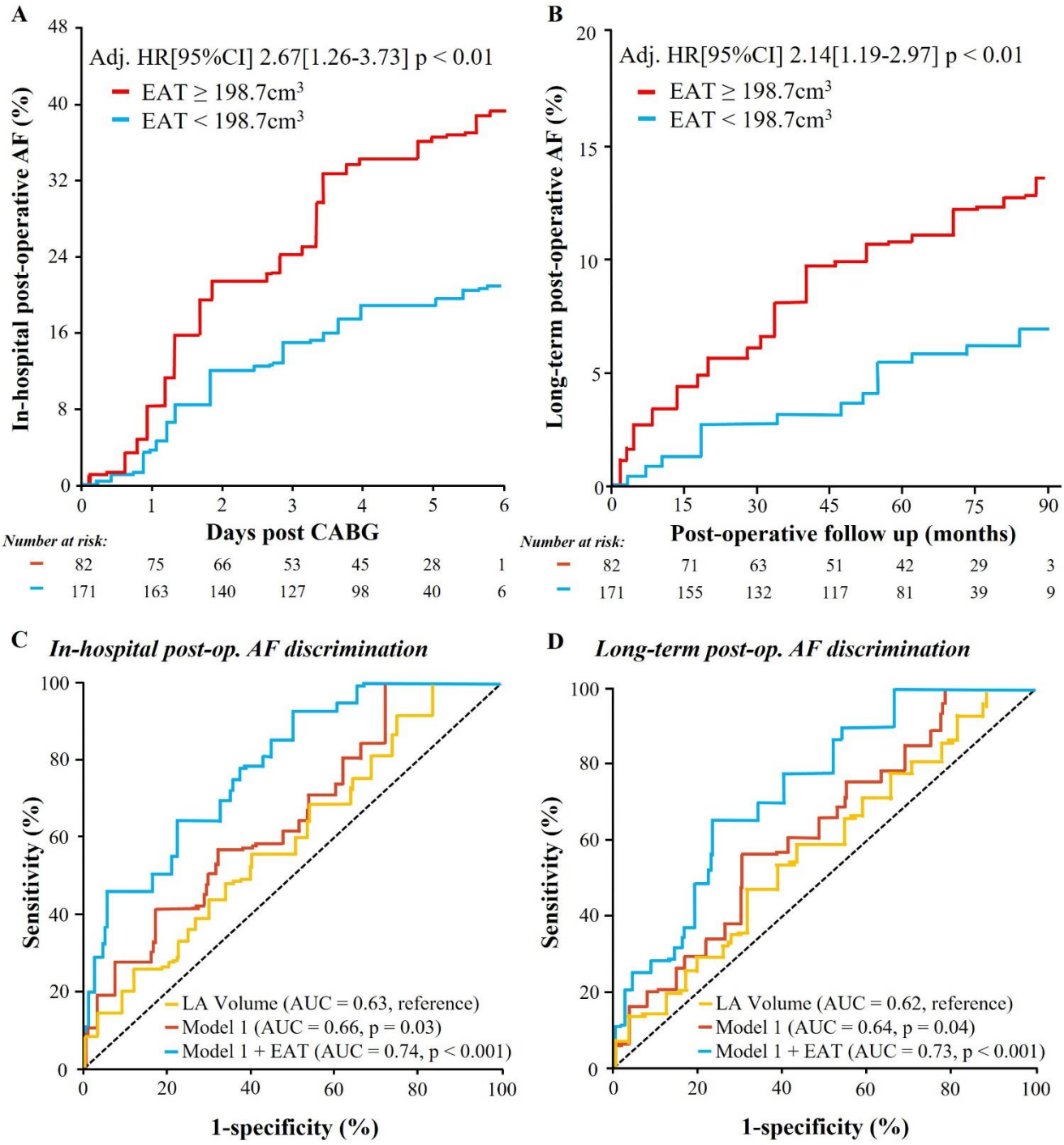

Figure 8. Prognostic value of EAT volume for post-operative AF

Kaplan-Meier curve and adjusted HR for in-hospital post-operative AF (A) and long-term post-operative AF (B), with sample dichotomised by Youden's J index derived cut-point of EAT volume (high risk ≥ 198.7cm^3; low risk < 198.7cm^3), expressed per 1 SD increase of EAT volume. Adjustment is made for age, gender, hypertension, diabetes, CAC score, and BMI. (C,D) Time-dependent ROC

curves for discrimination of in-hospital post operative AF (C) and long-term post-operative AF (D). CCTA-derived LA volume (yellow) is shown alone; model 1 (red) consists of age, gender, hypertension, diabetes, CAC score, and BMI. The addition of EAT volume into model 1 is demonstrated (blue).

AF: atrial fibrillation; AUC: area under curve; BMI: body mass index; CI: confidence interval; EAT: epicardial adipose tissue; HR: hazard ratio; LA: left atrium; MI: myocardial infarction; RFs: risk factors

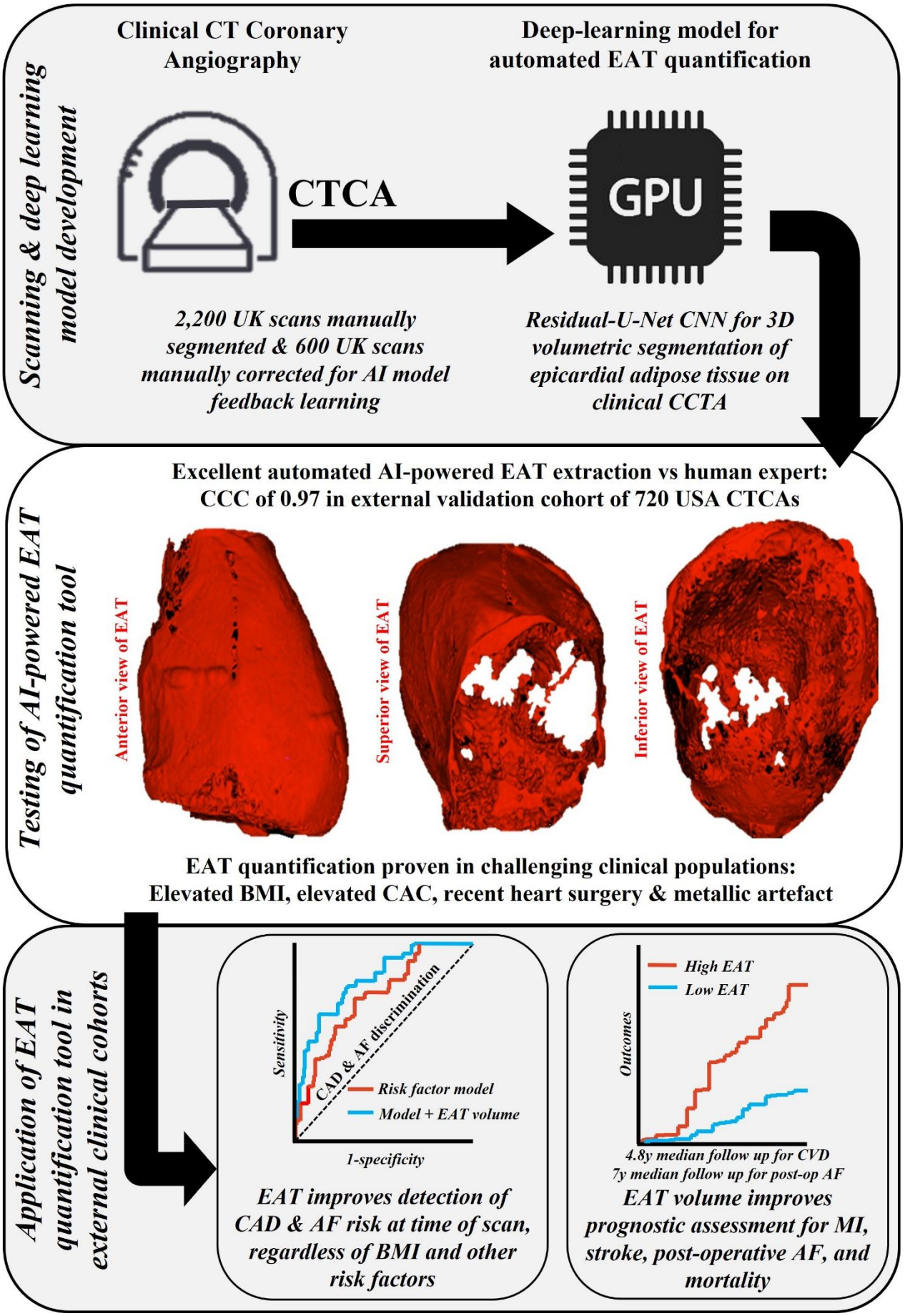
Scanning & deep learning model development
Clinical CT Coronary Angiography
Deep-learning model for automated EAT quantification
CTCA
GPU
2,200 UK scans manually segmented & 600 UK scans manually corrected for AI model feedback learning
Residual-U-Net CNN for 3D volumetric segmentation of epicardial adipose tissue on clinical CCTA
Testing of AI-powered EAT quantification tool
Excellent automated AI-powered EAT extraction vs human expert:
CCC of 0.97 in external validation cohort of 720 USA CTCAs
Anterior view of EAT
Superior view of EAT
Inferior view of EAT
EAT quantification proven in challenging clinical populations:
Elevated BMI, elevated CAC, recent heart surgery & metallic artefact
Application of EAT quantification tool in external clinical cohorts
Sensitivity
1-specificity
CAD & AF discrimination
Risk factor model
Model + EAT volume
EAT improves detection of CAD & AF risk at time of scan, regardless of BMI and other risk factors
High EAT
Low EAT
Outcomes
4.8y median follow up for CVD
7y median follow up for post-op AF
EAT volume improves prognostic assessment for MI, stroke, post-operative AF, and mortality

Central Illustration. The development, testing and external application of an AI-powered epicardial adipose tissue quantification tool for clinical practice

A deep-learning model was trained to automatically extract the adipose tissue from CCTA (top). The model performed excellently compared to human segmentation in internal and external testing, including in commonly occurring yet challenging CCTA patient groups (middle). The final automated AI-model for EAT quantification was applied to external clinical cohorts and revealed improved detection of prevalent disease risk for CAD and AF and provided incremental prognostic benefit for key cardiovascular events such as myocardial infarction, stroke, post-operative AF, and mortality in longitudinal cohorts.

AF: atrial fibrillation; AI: artificial intelligence; BMI: body mass index; CAC: coronary artery calcium; CAD: coronary artery disease; CT: computed tomography; CCTA: coronary computed tomography angiography; EAT: epicardial adipose tissue; GPU: graphics processing unit; MI: myocardial infarction.

Table 1. Demographics and scan characteristics of ORFAN Study cohorts used in AI model development and testing

		ORFAN *manual training cohort*	**ORFAN UK *feedback training cohort***	**ORFAN UK *internal validation cohort***	**ORFAN USA *external validation cohort***
Total number		2200	600	200	720
Age (years)		60 (50-70)	57 (49-64)	56 (48-62)	53 (43-62)
Male gender		1047 (47.6%)	315 (52.5%)	104 (52.0%)	389 (54.0%)
BMI (kg/m^2)		26.6 (23.6-29.9)	26.1 (23.1-30.0)	27.7 (24.8-30.7)	27.9 (24.5-32.2)
Active smoking		376 (17.0%)	93 (15.5%)	27 (13.5%)	N/A
Hypertension		711 (32.0%)	228 (38.0%)	73 (36.5%)	309 (42.9%)
Hypercholesterolaemia		896 (40.7%)	253 (42.2%)	76 (38.0%)	370 (51.4%)
Diabetes mellitus		286 (13.0%)	101 (16.8%)	25 (12.5%)	73 (10.1%)
Valve disease		139 (6.3%)	31 (5.2%)	13 (6.5%)	49 (6.8%)
Known CAD		188 (8.5%)	55 (9.2%)	21 (10.5%)	331 (46.0%)
Atrial fibrillation		98 (4.5%)	21 (3.5%)	9 (4.5%)	98 (13.6%)
Previous heart surgery		47 (2.1%)	19 (3.2%)	7 (3.5%)	16 (2.2%)
Scans					
Sites (scanner make & model)		Oxford, UK (GE Revolution GSI, GE Lightspeed VCT & Canon Aquilion One) Bath, UK (Siemens Drive) Milton Keynes, UK (Canon Aquilion Prime SP) Leicester, UK (Siemens Definition Flash)		Oxford, UK (GE Revolution GSI, GE Lightspeed VCT & Canon Aquilion One)	Cleveland, USA (Philips Brilliance iCT & Siemens Definition Flash)
Tube voltage					
	120 kVp	2112 (96.0%)	567 (94.5%)	193 (96.5%)	463 (64.3%)
	100 kVp	81 (3.7%)	33 (5.5%)	7 (3.5%)	257 (35.7%)
	80 kVp	7 (0.3%)	0 (0%)	0 (0%)	0 (0%)
EAT volume (cm^3)		133.2 (100.1-191.8)	124.9 (97.4-203.2)	120.9 (95.1-156.2)	169.3 (111.6-241.7)

BMI**:** Body mass index; CAD: Coronary artery disease; EAT: Epicardial adipose tissue; GE: General Electric.

Values expressed as n(%) or median(IQR)

Table 2. Demographics and scan characteristics of external clinical cohorts

		AdipoRedOx *cohort*	**SCOTHEART *cohort***
Total number		253	1558
Age (years)		67 (59-74)	58 (47-69)
Male gender		220 (87.0%)	887 (56.9%)
BMI (kg/m^2)		27.9 (25.0-31.1)	28.7 (25.1-33.2)
Active smoking		127 (50.2%)	298 (19.1%)
Hypertension		186 (73.5%)	541 (34.7%)
Hypercholesterolaemia		227 (89.7%)	810 (52.0%)
Diabetes mellitus		55 (21.7%)	173 (11.1%)
Valve disease		48 (19.0%)	144 (9.2%)
Known CAD		253 (100%)	158 (10.1%)
Atrial fibrillation		18 (7.1%)	32 (2.1%)
Previous heart surgery		253 (100%)	33 (2.1%)
Scans			
Site Scanner make & model		Oxford -GE Revolution GSI -GE Lightspeed VCT -Canon Aquilion One	Scotland -Philips Brilliance 64, -Siemens Biograph mCT -Canon Aquilion One
Tube voltage			
	120 kVp	253 (100%)	846 (54.3%)
	100 kVp	0 (0%)	712 (45.7%)
	80 kVp	0 (0%)	0 (0%)
EAT volume (cm^3)		162.9 (103.3-223.3)	130.1 (94.2-171.6)

BMI**:** Body mass index; CAD: Coronary artery disease; EAT: Epicardial adipose tissue; GE: General Electric. Values expressed as n(%) or median(IQR)

Deep-Learning for Epicardial Adipose Tissue Assessment with Computed Tomography: Implications for Cardiovascular Risk Prediction

West et al

SUPPLEMENTARY MATERIAL

Final as accepted

Supplementary Methods

Study ethics

All studies utilised in this manuscript complied with the human research ethics committees of the coordinating institute. The ORFAN Study (15/SC/0545) and the AdipoRedOx Study (C11/SC/0140) are sponsored by the University of Oxford and are both conducted with approval of the South Central – Oxford C Research Ethics Committee, as part of the Oxford Heart Vessels and Fat (ox-HVF) programme. The SCOT-HEART trial was sponsored by the University of Edinburgh and was conducted with the approval of the South-East Scotland Research Ethics Committee (NCT01149590). ORFAN USA sites research protocol was approved by all local institutional review boards, including material and data sharing agreements, with waiver of individual informed consent.

Study populations

ORFAN Study

The ORFAN Study is an Ox-HVF study that enrols adult patients who receive clinically indicated CCTA for all accepted indications at collaborating hospitals. Enrolment is through individual clinical sites and includes 13 NHS Trusts in England and two clinical sites in the USA. ORFAN scans utilised in this study were performed between January 2015 through to December 2020. For each patient included in the study the CCTA scan is pseudo-anonymised and delivered to The Oxford Academic Cardiovascular CT (OXACCT) Core Lab for analysis. 2,200 ORFAN patients' scans were utilised for the manual training of the deep-learning model while 600 further unseen scans were utilised for feedback learning (where the scan is fed into the model for automated segmentation, the output segmentation is then corrected by a human expert before being fed back into the model). 100 unseen UK ORFAN scans were utilised for preliminary evaluation of the model, and 200 unseen UK ORFAN scans were used for internal validation of the model. No outcome analysis of the ORFAN cohort was performed. 720 ORFAN USA scans (Cleveland Clinic, OH) were used only for external validation of the model and remained sequestered throughout the development and internal validation process.

AdipoRedOx Study

The AdipoRedOx study is an Ox-HVF study that enrols cardiac surgery patients at the Oxford University Hospitals NHS Foundation Trust, UK. The study is designed to investigate the role of inflammation and redox-state biology on heart disease through the collection of heart, vessel, and adipose tissue at the time of surgery. Relevant to this study, participants also undergo a CCTA within 6 weeks following surgery. Scans and relevant patient data from 253 participants were utilised in this study for the validation of the automated EAT quantification tool in challenging post-cardiac surgery patients.

SCOT-HEART trial

SCOT-HEART is an open-label, randomized, controlled, parallel-group trial that was performed at 12 centres across Scotland, commencing in 2009. Adult patients (n=4126) referred to outpatient cardiology clinics for stable chest pain were randomly assigned in a 1:1 ratio to standard care plus CCTA or to standard care alone. No standard-care patients were utilised in this study. The trial has been described in detail previously[1, 2]. The median duration of follow-up was 4.8 years. In this study, 1,558 eligible patients who had been randomised to the CCTA arm of the study were utilised.

Risk factors

In regression models, hypertension was defined based on the presence of a documented diagnosis or treatment with an antihypertensive regimen, according to the relevant clinical guidelines[3]. Similar criteria were applied for the definition of hypercholesterolemia and diabetes mellitus[4, 5]. Valve disease was defined as the presence of any documented aortic or mitral valve stenosis or regurgitation (of any severity), or previous valve repair and/or replacement procedure, including minimal invasive methods. Previous heart surgery was defined as any previous documented coronary artery bypass graft procedure or valve replacement or repair procedure (not including TAVI). Active smoking was defined as any documented active smoking of any amount of tobacco products, including all tobacco products. All SCOT-HEART baseline variables have been described in further detail elsewhere[6].

Outcomes

SCOT-HEART Study

The cross-sectional outcome of AF was defined as any documented diagnosis of paroxysmal, persistent or chronic AF within a patient's medical history, including self-report of the patient at the time of enrolment in the study. Outcomes within SCOT-HEART trial are all defined within the Study Protocol[6, 7]. Importantly, MI was defined as per the Universal Definition of the Joint ESC/ACCF/AHA/WHF Task Force for the Redefinition of Myocardial Infarction[8]. For the purposes of this study, the investigators followed the original SCOT-HEART investigators adjudication of events. This adjudication occurred according to the guidelines of the ACC/AHA[9] and the Academic Research Consortium for definition of the cause of death[10]. Cardiac mortality within the study was defined as 'any death due to proximate cardiac causes (e.g. myocardial infarction, low-output heart failure, fatal arrhythmia)'[6]. Sudden cardiac death was also included within this group[9, 10]. Any other death that was not captured by the previous definition was classified as of non-cardiac cause. Non-cardiac deaths included vascular causes such as stroke and embolism within the pulmonary circulation. Deaths were classified as 'deaths of unknown cause' only when information on the exact cause could not be obtained with certainty, which was at the discretion of the local SCOT-HEART investigators. The protocol of the SCOT-HEART study required that all adjudication of study events and cause of death be performed at each local site by the local study investigators. These investigators were not involved in the CT scan analysis or the statistical analysis of the study data. Events were ascertained via patient chart review, death certificate review and/or telephone follow-up or in-person verification with family members. No patient events were re-adjudicated for this study. All information utilised in this study was sent for statistical analysis to an independent team based at the University of Oxford, United Kingdom, which performed all analyses blind to scan data.

AdipoRedOx Study

Immediate post-operative AF outcomes were collected in hospital during the in-patient stay following the surgery. AF in this context was defined as >30s of AF captured on continuous electrocardiographic monitoring. Patients were on telemetry monitoring of heart rhythm throughout their in-patient stay. If telemetry was ceased by the treating team, the patient was censored at that time in analysis.

The long-term post-operative AF outcome was collected from NHS Digital data via linkage with study participant identifiers (NHS number and date of birth). Linkage was made to hospital episode statistics data for all regular admissions, outpatient episodes, emergency presentations and critical care episodes following the surgery. The long-term AF outcome is a merger of relevant ICD-10 codes for AF including codes that capture the diagnosis of paroxysmal AF, persistent AF, chronic AF and AF unspecified (codes I48.0, I48.1, I48.2, I48.9, respectively). If any of these codes were entered for a patient over the follow-up period, this was counted as an event.

Manual CCTA segmentation

All analyses were performed using the standard operating procedures of the Oxford Academic Cardiovascular CT (OXACCT) core lab at the Acute Vascular Imaging Centre (AVIC) in the University of Oxford. Manual segmentation of the whole heart and the pericardium was performed on randomly selected ORFAN CCTA scans for the training of the deep-learning model. The manual segmentation was undertaken by 2 independent readers. Both readers are trained members of the OXACCT Core Lab and have undertaken training in the specific whole heart segmentation technique required. The training of the readers was overseen by the Director of the Core Lab (SCCT level 3 qualification). According to the Quality Management System of the OXACCT core lab, the readers receive training based on a well-defined and controlled SOP. Before qualification as expert readers, the core lab members need to achieve <5% variability in manual segmentation of the pericardium compared to the gold standard segmentations included into the training and testing package, and they perform at least 150 supervised manual segmentations with assessment and peer-review prior to commencing any research analysis. The standard operating procedures of the Core Lab mandate the use of quality control assessment of segmentations performed for both research and industry.

The whole heart within the pericardium was segmented between the bifurcation of the pulmonary trunk superiorly and the apex of the pericardium inferiorly. CaRi-Heart® version 2.2.1 (Caristo Diagnostics Ltd., Oxford, UK) was utilised for manual imaging segmentation (See Supplementary Figure 1 for example of manual segmentation). All voxels within the pericardium including the visceral pericardium were included. Examination of EAT volume segments for intra-observer bias was excellent with both expert human readers having excellent intra-class correlation coefficient in a test of 20 blinded repeat reads of the same case (reader 1, ICC[95%CI] = 0.987[0.980-0.999] $p < 0.001$; reader 2, 0.984[0.976-0.998] $p < 0.001$; interval between reads 2 weeks). Following initial training with 2200 manually segmented CCTA, the model was further enhanced by 3 iterations of feedback learning performed on unseen CCTA scans from the ORFAN study. These unseen scans were fed into the model in batches of 200, then the output segmentations were manually corrected by 2 experts readers (same readers as the training analysis) before being fed back into the deep-learning model.

The extraction of EAT volume from the heart segmentation

The extraction of EAT volumes from the segmentation of the whole heart was achieved by automated selection of adipose tissue voxels. The Hounsfield unit (HU) range of -190 HU through to -30 HU was utilised, adhering to the conventional definition of

adipose tissue density on CCTA[11-13]. The extraction of the EAT volume on a per-voxel basis from within the whole heart segment was fully automated in a bespoke module within the CaRi-Heart® platform, created especially for the purpose of the quantification of EAT from CT segmentations. An example of EAT segmentation is shown in Figure 3B, with manual segmentations and automated segmentation shown independently, and merged.

Traditional CCTA interpretation methods

CAC Score

In the SCOT-HEART Trial population coronary artery calcium score was quantified by the Agatston method on non-contrast cardiac CT scans using commercially available software (Aquarius Workstation® V.4.4.11-13, TeraRecon Inc., Foster City, CA, USA), in those patients with an indication for CCS assessment.

Obstructive CAD

Included SCOT-HEART trial scans has been previously reviewed by two independent clinical researchers within the OXACCT Core Lab, as published previously[14]. Obstructive CAD was defined as the presence of at least one coronary stenosis ≥50% on CCTA.

Coronary computed tomography angiography technical parameters

ORFAN Study

Participants in the ORFAN study in the UK underwent CCTA scans at NHS Trust hospitals including Oxford University Hospital NHS Foundation Trust, University Hospitals of Leicester NHS Trust, Royal United Hospitals Bath NHS Foundation Trust, Milton Keynes University Hospital NHS Foundation Trust. All scans were performed according to local clinical procedures, with minimal variance between sites. Heart rate was optimised using intravenous injection of beta-blockers and sublingual glyceryl-trinitrate (800ug) was also administered to achieve maximum coronary vasodilatation if needed. CCTA was performed following intravenous injection of 50-70 ml of iodine based contrast medium (typically Niopam 370, BRACCO UK Ltd) at a flow rate rate of 5.5-6.5 mL/sec (axial slice thickness on Canon scanners was typically 0.5mm, with Siemens typically between 0.65mm or 0.75mm, rotation time was 0.35 sec, detector coverage was up to 160mm and tube energy selected based on body habitus and according to local clinical practice). Prospective image acquisition was used by ECG-gating at 75% of cardiac cycle (with 100msec padding if required). If not possible, retrospective image acquisition was used (e.g. in the presence of irregular rhythm). For ORFAN USA sites, a total of 2,246 scans were available for inclusion. A random selection of 720 were selected for inclusion in the cohort. The majority of the CCTA scans (n=627, 87·0% of the total number of scans) were performed in a 256-slice Brilliance iCT scanner (Philips Medical Systems, Best, Netherlands), with the remainder using a 2 x 128-slice Definition Flash scanner (Siemens Healthcare, Erlangen, Germany) (n=70, 9.7%) and a 2 x 192-slice Somatom Force CT scanner (Siemens Healthcare, Forchheim, Germany) (n=23, 3·2%). In patients with heart rate > 60 beats/minute, 5 mg of intravenous metoprolol (with incremental 5 mg doses up to a maximum dose of 30 mg) or intravenous diltiazem (5 mg increments up to 20 mg maximum), if the heart rate remained above 60 beats per minute once the patient was positioned on the CT table. Patients also received 0·3 mg of nitroglycerin sublingually immediately before CCTA and iodinated contrast (Omnipaque 350, General Electric, Milwaukee, USA) was administered at flow rate of 5-6 ml/s.

For all ORFAN sites, scans with profoundly poor-quality images, more than 2 missing slices, severe beam hardening or significant step artifacts were excluded from the analysis. Minor to moderate scan artefacts were acceptable and included in analysis.

AdipoRedOx Study

Participants in AdipoRedOx underwent CCTA using a 64-slice scanner (LightSpeed VCT, General Electric), as previously described.[15] Heart rate was optimised using intravenous injection of beta-blockers and sublingual glyceryl-trinitrate (800ug) was also administered to achieve maximum coronary vasodilatation. A non-contrast prospectively ECG triggered axial acquisition CT scan was obtained (0.35 sec rotation time, 2.5 mm axial slice thickness, 20 mm detector coverage, tube energy of 120 kV and 200 mA) with the carina and the diaphragm used as cranial and caudal landmarks respectively. Lung field of view was extended to cover the entire thoracic soft tissue (for subcutaneous adipose tissue analysis). CCTA was performed following intravenous injection of 95ml of iodine based contrast medium (Niopam 370, BRACCO) at a flow rate rate of 4.5-6mL/sec (tube energy of 120 kVp, axial slice thickness of 0.625 mm, rotation time of 0.35 sec, detector coverage of 40 mm). Prospective image acquisition was used by ECG-gating at 75% of cardiac cycle (with 100 msec padding for optimal imaging of the right coronary artery if required). There were no exclusions from the AdipoRedOx cohort based on scan parameters.

SCOT-HEART trial

CCTA scans were performed using either two 64 detector row scanners (Brilliance 64, Philips Medical Systems, Netherlands, and Biograph mCT, Siemens, Germany) or one 320 detector row scanner (Aquilion ONE, Toshiba Medical Systems, Japan) at three imaging sites according to each site's local protocol[1, 2]. A total of 1786 patients were available for analysis. Scans performed at tube voltage settings other than 100 or 120 kVp, and scans with profoundly poor-quality images (unsuitable for human or machine analysis), 2 or more missing slices, severe beam hardening or significant step artifacts were excluded from the analysis (n=228), resulting in a study dataset of 1558 CCTA scans.

Scan retrieval

All CCTAs from each study were first anonymized locally, or in the cloud at the time of transfer, and sent to the Oxford Academic Cardiovascular Computed Tomography (OXACCT) core lab (Oxford, UK) for either manual analysis on dedicated workstations or for sequestering for later automated validation analysis.

The training of the deep-learning model for automated segmentation of the whole heart within the pericardium

The 2,200 manually whole heart segmented CCTA scans were individually normalised to have zero mean and unary standard deviation, as on input networks performed better in this intensity range. A convolutional neural network was used for segmentation by casting them to voxel-wise classification. The network was trained to predict whether the central voxel of a patch is or is not within the bounds of the pericardium depending on the content of the surrounding 3D patch.

A fully automatic method was employed using 3D Residual-U-Net neural network architecture [3] for 3D volumetric segmentation of CCTA data. A building block of a Residual-U-Net is called a residual block or skip connection. The activation of a layer is fast-forwarded to a deeper layer in the neural network in a residual block. This allows training much deeper neural networks without the issue of vanishing gradients. The architecture resembles auto encoder framework and consist of 4 down-sampling and 4 up-sampling blocks which are connected by a bridge block. Feature size is halved after passing through every

down-sampling block by a max-pooling layer at its base. At the beginning of every up-sampling block the feature size is doubled using transposed convolution layer with stride of size 2 for each dimension. Passing information through interconnections was achieved by using zero padding. After every convolution operation we fill the newly computed vector with zeros to its original length and therefore both convolution layers use the same size of the input vector. During training, the parameters of the kernels were optimized using Adam optimizer, with the target of minimizing the error between the predictions and the true labels. The hyper-parameters of the network were tuned following the first and second stages of the feedback learning process, that is after he first and second cycles of scan (n=200) input and correction.

The CNN as shown in Figure 3A of the main text demonstrates the layers of model. The light green boxes (Conv+RelU) represent a convolutional layer. These layers capture the spatial relationship between CCTA voxels to receive image features using small patches of input data by learning local connectivity patterns followed by RelU activation to ensure non-linearity, sparsity, and a reduced likelihood of vanishing gradient. Yellow boxes (Concat) represents residual interconnections to allow gradients to pass through the network directly by skipping over series' of convolution and non-linear activation functions to solve the degradation problem of the deep networks, and concatenation to add tensors of both connections. Max pooling layer is represented by dark green colour box (MaxPool) to extract sharp and smooth features. Orange boxes (UnPool) represents the up-sampling step to revert the effect of the max pooling operation. The purple box (Sigmoid) represents the output layer using sigmoid function. This outputs values in the range 0 to 1 representing the probability of a voxel being within the desired segmentation of the heart pericardium. The grey horizontal lines represent concatenation of decoder paths with the corresponding feature map from the encoder path.

The network architecture was trained using Keras framework using Tensorflow 2.2 (Google Brain, Mountain View, CA, USA) as backend. The network used a binary cross-entropy as a loss function and Dice coefficient as performance metric.

Automated left atrium segmentation

Left atrium volume was utilised as a co-variate in analysis of the relationship between EAT volume and post-operative AF risk within the AdipoRedOx Study. In the AdipoRedox Study LA volume was calculated via automated quantification upon the same CCTA utilised for EAT quantification. The automated segmentation was trained in the same manner to the whole heart segmentation – via a Residual-U-Net neural network architecture for 3D volumetric segmentation the LA chamber, including the LAA. The training cohort for this analysis was the same as described for the whole heart in this manuscript – the UK ORFAN Study population. The internal validation cohort was 200 unseen UK ORFAN scans, with resulting concordance correlation coefficient (CCC) for human vs machine of 0.981. The external validation cohort was in 720 USA ORFAN CCTAs, with a CCC of 0.971. No AdipoRedOx Study scans were utilised in the training or validation of the LA volume quantification tool. The automated tool was incorporated into the CaRi-Heart analysis platform (Caristo Diagnostics Ltd., Oxford, UK).

Preliminary internal validation of the whole heart segmentation DLN

EAT was segmented manually in 100 randomly selected scans from the UK arm of ORFAN, all previously sequestered from the algorithm, prior to the same set of scans being segmented by the automated deep-learning algorithm. This analysis occurred prior to the initiation of the feedback learning cycles and represents a preliminary validation of the model (Supplementary Figure 2).

CCC was excellent between human expert and the machine at 0.960, and the bias was non-significant at 5.5[-8.0-14.7]cm^3, p = 0.22.

For the whole heart volume in the same 100 scans there was minimal variability between a single human expert and machine (Supplementary Figure 3). CCC was excellent between human expert and the machine at 0.969, and the bias was non-significant at 29.2[-30.3-77.5]cm^3, p = 0.18.

Quantification of blood markers

AdipoRedOx

NT-proBNP was calculated from blood samples collected in an EDTA tube intra-operatively for each participant. Plasma BNP was quantified by chemiluminescent-microparticle immunoassay (Architect BNP, Abbott, Germany).

SCOT-HEART Trial

Non-HDL cholesterol was calculated along with a complete lipid panel as previously described[6, 7].

Supplementary statistical analysis

Participant demographics are summarized as numbers (percentages) or median (25th to 75th percentile) for categorical and continuous variables, respectively. For intra-observer repeatability, intraclass correlation coefficient was calculated with 20 repeat cases per reader.

Whenever utilised, coronary artery calcium (CAC) score was log-transformed before inclusion in regression models (ln[CAC + 1]).

For cross-sectional analysis of disease risk conveyed by EAT volume, multiple-adjusted logistic regression was used for calculation of the odds-ratio of prevalent disease (AF at time of CCTA and obstructive CAD from CCTA) at the time of the CCTA given increase in EAT by one standard deviation (SD). Within the main text, results are presented with adjustment for all models with a uniform set of co-variates. Supplementary results are presented with a statistical approach to risk factor adjustment. Longitudinal assessment of the prognostic value of EAT volume was performed by multivariable Cox regression. Both odds ratios and hazard ratios are reported per one SD increase in EAT volume. The variables that are included in each supplementary model of the SCOT-HEART trial analysis are the risk factors that have shown a statistically meaningful association with the relevant outcome (dependent variable) in univariate analysis, at the level of $p \leq 0.1$ (see Supplementary Table 1).

When calculating Youden's J Statistic within the SCOT-HEART cohort, we weighted the influence of each outcome (all-cause mortality, fatal/non-fatal MI and fatal/non-fatal stroke) according to the number of events in the population and then tested the prognostic value of the high vs low EAT volume (as a dichotomous variable) by multivariable Cox regression analysis after adjustment for relevant disease risk factors as listed in the results.

For analysis of risk of post-operative AF in CABG patients from the AdipoRedOx Study, secondary analysis with AF specific risk factors was performed (see Supplementary Figure 6). The risk factors selected in this analysis were selected for their known relationship with new onset AF in the post-operative population following literature review.

Statistical analyses were performed predominantly in STATA SE version 15 (Stata Corp, College Station, TX, USA), with some analysis in the *R* environment (*R for* Windows 4.0.4). All tests were two-sided and α was set at 0.05, unless specified otherwise.

Supplementary results

Preliminary internal validation of the automated whole heart and EAT volume detection model vs human segmentation

EAT was segmented manually in 100 randomly selected scans from the UK arm of ORFAN, all previously sequestered from the algorithm, prior to the same set of scans being segmented by the automated deep-learning algorithm. This analysis occurred prior to the initiation of the feedback learning cycles and represents a preliminary validation of the model (Supplementary Figure 1). CCC was excellent between human expert and the machine at 0.960, and the bias was non-significant at 5.5[-8.0-14.7]cm^3, p = 0.22.

For the whole heart volume in the same 100 scans there was minimal variability between a single human expert and machine (Supplementary Figure 2). CCC was excellent between human expert and the machine at 0.969, and the bias was non-significant at 29.2[-30.3-77.5]cm^3, p = 0.18.

Cross-sectional clinical correlations with statistical approach to co-variate selection

At the time of the CCTA, application of the fully automated segmentation tool for quantification of EAT volume was found to be a significant independent predictor of the presence of AF at time of CCTA and obstructive CAD from CCTA (any one coronary vessel with ≥50% stenosis on CCTA), within 1,558 patients randomised to receive CCTA in the SCOT-HEART trial population. When accounting for AF risk factors the odds ratio (OR[95%CI]) of AF at time of CCTA per 1 standard deviation (SD) increase of EAT was 1.20[1.06-1.45] p=0.03 (Supplementary Figure 4A). When accounting for CAD risk factors the OR of obstructive CAD from the CCTA per 1 SD increase of EAT was 1.12[1.03-1.30] p=0.01 (Supplementary Figure 4B).

Longitudinal EAT volume clinical correlations with statistical approach to co-variate selection

Median follow up for the 1,558 patients randomised to receive CCTA in SCOT-HEART which were analysed was 4.8 years. There were 35 deaths of all causes (2.25%) of which 4 (0.25%) were deaths related with coronary heart disease. There were 8 fatal/non-fatal strokes (0.51%) and 39 fatal/non-fatal myocardial infarctions (2.5%).

The hazard ratio (HR[95%CI]) of all-cause mortality per 1 SD increase of EAT was 1.24[1.08-1.34] p=0.03, after accounting for relevant general disease risk factors (Figure 6C). When adjusted for the same risk factors as Figure 6A, the HR[95%CI] of non-cardiac mortality per 1 SD increase of EAT volume was 1.14[1.02-1.37] p=0.04 (Supplementary Figure 4D). This constitutes a ΔHR of -0.10, confirming that EAT is a measure of visceral adipose tissue related with multiple fatal pathologies, unrelated to CAD. When accounting for CAD risk factors the HR of fatal/non-fatal MI per 1 SD increase of EAT was 1.25[1.08-1.45] p=0.001 (Supplementary Figure 4E). Finally, when accounting for stroke risk factors the HR[95%CI] of fatal/non-fatal stroke per 1 SD increase of EAT is 1.12[1.03-1.27] p=0.02 (Supplementary Figure 4F).

EAT volume and post-operative atrial fibrillation risk with AF specific risk factors

As is reported in the main manuscript, utilising 250 scans from patients in the AdipoRedOx Study, the longitudinal associations between EAT volume and in-patient post-operative AF and long-term AF following surgery were investigated.

Utilising the same methods described in the main text, secondary analysis was performed with multivariable adjustment for relevant AF risk factors including LA volume and NT-proBNP (see above in Supplementary Methods for quantification details). High EAT volumes were associated with a significantly greater risk for in-patient post-operative AF following adjustment for typical AF risk factors, with HR[95%CI] of 1.54[1.12-3.33] p<0.01, per 1 SD increase in EAT volume (Supplementary Figure

6A). Equally, for long-term new-onset AF following cardiac surgery high risk EAT volumes were associated with a significantly greater risk for long-term AF following adjustment for typical AF risk factors, with HR[95%CI] of 1.34[1.10-2.87] p<0.01, per 1 SD increase in EAT volume (Supplementary Figure 6B).

The addition of EAT volume into a clinical risk factor model, significantly improved the prediction of new-onset in-hospital AF in ROC curve analysis (Supplementary Figure 6C) with ΔAUC of +0.108 (p<0.01) for risk factor model 1 with the addition of EAT volume, and ΔAUC of +0.221 (p<0.001) with the addition of the risk factor model plus EAT volume on top of CCTA derived LA volume alone. The same was found for new-onset long-term AF (Supplementary Figure 6D), with ΔAUC of +0.09 (p<0.001) for risk factor model 1 with the addition of EAT volume, and ΔAUC of +0.141 (p<0.001) over LA volume alone.

EAT volume and post-operative atrial fibrillation risk with waist-hip ratio included in analysis

Replacement of BMI with waist-hip ratio (WHR) in the original analysis as presented in Figure 8 did not alter the statistical significance of the results (Supplementary Figure 7). High EAT volumes were associated with a significantly greater risk for in-patient post-operative AF following adjustment for CVD risk factors including WHR, with HR[95%CI] of 12.57[1.23-3.63] p<0.01, per 1 SD increase in EAT volume (Supplementary Figure 7A). Equally, for long-term new-onset AF following cardiac surgery high risk EAT volumes were associated with a significantly greater risk for long-term AF following adjustment for CVD risk factors including WHR, with HR[95%CI] of 2.16[1.11-3.21] p<0.01, per 1 SD increase in EAT volume (Supplementary Figure 7B). The addition of EAT volume into a clinical risk factor model including WHR, significantly improved the prediction of new-onset in-hospital AF in ROC curve analysis (Supplementary Figure 7C) with ΔAUC of +0.05 (p<0.01) for risk factor model 1 with the addition of EAT volume, and ΔAUC of +0.09 (p<0.001) with the addition of the risk factor model plus EAT volume on top of CCTA derived LA volume alone. The same was found for new-onset long-term AF (Supplementary Figure 7D), with ΔAUC of +0.07 (p<0.01) for risk factor model 1 with the addition of EAT volume, and ΔAUC of +0.1 (p<0.001) over LA volume alone.

Supplementary Tables

Supplementary Table 1. Standardised univariate analysis of variables for inclusion in multivariable models in addition to EAT volume			
Variables		***Beta***	***P-value****
Dependent variable: Presence of atrial fibrillation at the time of the CCTA			
Factors (independent variables) qualified for inclusion in the models			
	Age	0.32	0.002
	Male gender	0.19	0.005
	BMI	0.16	0.01
	Hypertension	0.15	0.009
	Diabetes	0.09	0.05
	Valve disease	0.10	0.09
	Previous heart surgery	0.06	0.07
Factors (independent variables) tested but not qualified for inclusion in the models			
	Non-HDL cholesterol	-0.02	0.34
	Active smoker	0.03	0.20
	Previous smoking history	-0.02	0.55
	Obstructive disease from CCTA	0.19	0.21
	CAC Score	0.09	0.49
Dependent variable: Obstructive CAD from CCTA (cross-sectional)			
Factors (independent variables) qualified for inclusion in the models			
	Age	0.27	0.002
	Male gender	0.17	0.005
	BMI	0.19	0.009
	Hypertension	0.17	0.01
	CAC Score	0.18	0.01
	Non-HDL Cholesterol	0.10	0.02
	Active smoker	0.07	0.04
Factors (independent variables) tested but not qualified for inclusion in the models			
	Diabetes	0.04	0.22
	Valve disease	0.01	0.53
	Previous cardiac surgery	0.04	0.29
	Previous smoking history	0.09	0.19
Dependent variable: All-Cause Mortality			
Factors (independent variables) qualified for inclusion in the models			
	Age	0.31	0.002
	Male gender	0.19	0.01
	BMI	0.19	0.04
	Hypertension	0.09	0.05
	Diabetes	0.10	0.09
	Active smoker	0.09	0.06
Factors (independent variables) tested but not qualified for inclusion in the models			
	Non-HDL Cholesterol	0.08	0.22
	CAC Score	-0.05	0.38
	Obstructive disease from CCTA	0.08	0.25
	Valve disease	0.04	0.34
	Previous cardiac surgery	0.009	0.58
	Previous smoking history	0.11	0.15
Dependent variable: Non-cardiac Mortality			
Factors (independent variables) qualified for inclusion in the models			
	Age	0.36	0.001
	Male gender	0.12	0.01
	BMI	0.09	0.04
	Hypertension	0.03	0.09
	Diabetes	0.13	0.07
Factors (independent variables) tested but not qualified for inclusion in the models			
	Non-HDL Cholesterol	0.03	0.28
	CAC Score	-0.11	0.19
	Obstructive disease from CCTA	0.03	0.22
	Valve disease	0.10	0.33
	Previous cardiac surgery	0.04	0.48
	Active smoker	0.11	0.15
	Previous smoking history	0.09	0.18

Dependent variable: MI			
Factors (independent variables) qualified for inclusion in the models			
	Age	0.31	0.008
	Male gender	0.09	0.09
	BMI	0.15	0.02
	Hypertension	0.11	0.05
	Non-HDL Cholesterol	0.09	0.08
	CAC Score	0.13	0.09
	Obstructive disease from CCTA	0.16	0.04
Factors (independent variables) tested but not qualified for inclusion in the models			
	Diabetes	0.06	0.08
	Valve disease	0.03	0.45
	Previous cardiac surgery	-0.05	0.34
	Active smoker	0.12	0.15
	Previous smoking history	0.009	0.22
Dependent variable: Stroke			
Factors (independent variables) qualified for inclusion in the models			
	Age	0.30	0.009
	Male gender	0.12	0.02
	BMI	0.16	0.01
	Hypertension	0.09	0.02
	Valve disease	0.07	0.08
	Previous heart surgery	0.16	0.06
Factors (independent variables) tested but not qualified for inclusion in the models			
	Diabetes	0.07	0.12
	Non-HDL cholesterol	0.003	0.66
	Active smoker	0.12	0.13
	Previous smoking history	0.02	0.46
	Obstructive disease from CCTA	0.006	0.59
	CAC Score	0.04	0.49

*Significance set at $p \leq 0.1$

AF: atrial fibrillation; BMI: body mass index; CAC: coronary artery calcium score; HDL: high-density lipoprotein; MI: myocardial infarction

Supplementary Table 2. Outcomes from the prospective clinical cohorts		
Prospective follow-up		
	AdipoRedOx ***cohort of cardiac surgery***	**SCOTHEART** ***outcomes cohort***
Duration in-hospital (days)	6 days (4.1-7.5)	N/A
Duration long-term follow up (months)	5.6 years (3.8-6.5)	4.8 years (4.2-5.7)
All-cause mortality	N/A	35 (2.25%)
Cardiac mortality	N/A	4 (0.26%)
Myocardial infarction*	N/A	39 (2.5%)
Stroke*	N/A	8 (0.51%)
Post-operative AF in hospital	97 (38.3%)	N/A
Post-operative AF long-term	48 (19%)	N/A

Data are median (IQR) or mean (%).
* Fatal and non-fatal.
AF: Atrial fibrillation; MI: myocardial infarction

ORFAN Study Investigators

Chief Investigator: Professor Charalambos Antoniades[1]

Investigators:

Dr Henry West[1]

Dr Alexios Antonopoulos[1]

Ms Sheena Thomas[1]

Ms Maria Lyasheva[1]

Dr Evangelos Oikonomou[1]

Dr Nikant Sabharwal[2]

Dr Cheerag Shirodaria[2]

Dr Susan Anthony[2]

Dr Andrew Kelion[2]

Prof Adrian Banning[2]

Dr Rafail Angelos Kotronias1,2

Dr Cheng Xie[1,2]

Dr Rajesh Kumar Kharbanda[1,2]

Dr Attila Kardos[1,4]

Dr David Adlam[3]

Dr Amrita Bajaj[3]

Dr Intrajeet Das[3]

Dr Aparna Deshpande[3]

Dr Praveen Rao[3]

Dr Tarun Mittal[5]

Dr Saeed Mirsadraee[5]

Dr Edward Nicol[5]

Dr Jonathan Rodrigues[6]

Dr Benjamin Hudson[6]

Prof John Greenwood[7]

Prof Colin Berry[8,9]

Prof Stephan Achenbach[10]

Dr Mohamed Marwan[10]

Dr Milind Y Desai[11]

Dr Nicholas Screaton[12]

Dr Pál Maurovich-Horvat[13]

Prof Guo-Wei He[14]

Dr Wen-Hua Lin[14]

Dr Li-Juan Fan[14]

Prof Naohiko Takahashi[15]

Dr Hidekazu Kondo[15]

Dr Neng Dai[16]

Prof. Junbo Ge[16]

Prof Bon-Kwon Koo[17]

Dr Gianluca Pontone[18]

Dr Marco Guglielmo[18]

Prof Ron Blankstein[19,20]

Prof Theodora Benedek[21]

Dr Ronak Rajani[22]

Dr Mak Sze Mun[22]

Dr Giulia Benedetti[22]

Dr Rebecca Louise Preston[22]

Dr Elisa McAlindon[23]

Dr Shahzad Munir[23]

Dr Derek Leslie Connolly[24]

Dr William Bradlow[25,26]

Dr Matthias Schmitt[27,28]

Dr Fabiano Serfaty[29]

Dr Ilan Gottlieb[30]

Prof Mario Fritsch T. Neves[31]

Prof David Ernest Newby[32]

Prof Steffen E Petersen[33,34]

Dr Francesca Pugliese[35]

Dr Nehal N Mehta[36]

Prof Stéphane Hatem[37]

Prof Alban Redheuil[38]

Dr Georgios Benetos[39]

Prof Meinrad Beer[40]

Dr Gastón A Rodríguez-Granillo[41]

Prof Joseph Selvanayagam[42]

Prof Bernard Gersh[43]

Dr Francisco Lopez-Jimenez[43]

Dr Ruben De Bosscher[44]

Dr Alain Tavildari[45]

Prof Gemma Figtree[46]

Dr Ibrahim Danad[47]

Dr Ronney Shantouf[48]

Dr Bas Kietselaer[49]

Prof Dimitris Tousoulis[50]

Prof George Dangas[51]

Prof Stefan Neubauer[1]

Prof John Deanfield[52,53]

Prof Keith Channon[1]

Investigator Affiliations:

1. Division of Cardiovascular Medicine, Radcliffe Department of Medicine, University of Oxford, UK
2. Oxford University Hospitals NHS Foundation Trust, Oxford, UK
3. Department of Cardiovascular Sciences & NIHR Leicester Biomedical Research Centre, University of Leicester, UK
4. Milton Keynes University Hospital NHS Foundation Trust, UK
5. Royal Brompton and Harefield NHS Foundation Trust, UK
6. Royal United Hospitals Bath NHS Foundation Trust & Department of Health, University of Bath, UK
7. Leeds Teaching Hospitals NHS Foundation Trust, UK
8. NHS Greater Glasgow and Clyde, NHS Scotland, UK
9. Golden Jubilee National Hospital, NHS Scotland, UK
10. Department of Cardiology, Friedrich-Alexander-Universität Erlangen-Nürnberg, Erlangen, Germany
11. Cleveland Clinic Heart and Vascular Institute, Cleveland, U.S.A
12. Royal Papworth Hospital NHS Trust, Cambridge, UK
13. Department of Radiology, MTA-SE Cardiovascular Imaging Research Group, Budapest, Hungary
14. TEDA International Cardiovascular Hospital, Tianjin, China
15. Oita University, Japan
16. Fudan University, China
17. Seoul National University, Seoul, South Korea
18. Centro Cardiologico Monzino IRCCS, University of Milan, Italy
19. Harvard Medical School, Boston, USA
20. Brigham and Women's Hospital, Boston, USA
21. University of Medicine and Pharmacy of Tirgu Mures, Romania
22. Guy's and St Thomas' NHS Foundation Trust, UK
23. Heart and Lung Centre, New Cross Hospital, Wolverhampton, UK
24. Sandwell & West Birmingham Hospitals NHS Trust, UK
25. University Hospitals Birmingham (UHB) NHS Trust, UK
26. University of Birmingham, UK
27. University Hospital of Manchester Foundation Trust, Manchester, UK
28. University of Manchester, Manchester, UK
29. Serfaty Clinicas, Rio de Janeiro, Brazil
30. Casa de Saúde São José, Rio de Janeiro, Brazil
31. Universidade do Estado do Rio de Janeiro, Rio de Janeiro, Brazil
32. University of Edinburgh, Royal Infirmary, Edinburgh, UK
33. The William Harvey Research Institute, Barts and The London School of Medicine and Dentistry, Queen Mary University of London, UK
34. Bart's Heart Centre, Barts Health NHS Trust, UK
35. NIHR Barts Cardiovascular Biomedical Research Centre, the William Harvey Research Institute, Queen Mary University of London & Barts Health NHS Trust, UK
36. National Institutes of Health, National Heart, Lung, and Blood Institute, USA
37. Foundation for Innovation in Cardiometabolism and Nutrition (ICAN), Paris, France
38. Sorbonne Université, Faculté de Médecine Pierre et Marie Curie, La Pitié Salpêtrière AP-HP, Paris, France
39. Lefkos Stavros Clinic Athens, Greece
40. Universitätsklinikum Ulm, Germany
41. ENERI Medical Institute, Buenos Aires, Argentina
42. South Australia Health and Medical Research Institute, Adelaide, Australia
43. Mayo Clinic, Rochester, USA
44. University Hospitals Leuven, Belgium
45. Cardiovista, France
46. University of Sydney, Australia
47. Amsterdam University Medical Centers, Netherlands
48. Cleveland Clinic Abu Dhabi, UAE
49. Zuyderland Medical Centre, Heerlen, Netherlands
50. University of Athens, Greece
51. Mount Sinai School of Medicine, New York, USA
52. University College London, UK
53. National Institute of Cardiovascular Outcomes Research (NICOR), UK

Supplementary Figures

Supplementary Figure 1. Preliminary internal validation of the deep-learning model for EAT volume segmentation

Following initial training of the model but prior to three iterations of feedback learning the model was assessed for preliminary performance against human expert segmentation on unseen CCTA. The scatterplot (A) and Bland-Altman plot (B) demonstrate the variability in EAT volume quantification between automated deep-learning machine and human expert analyst.

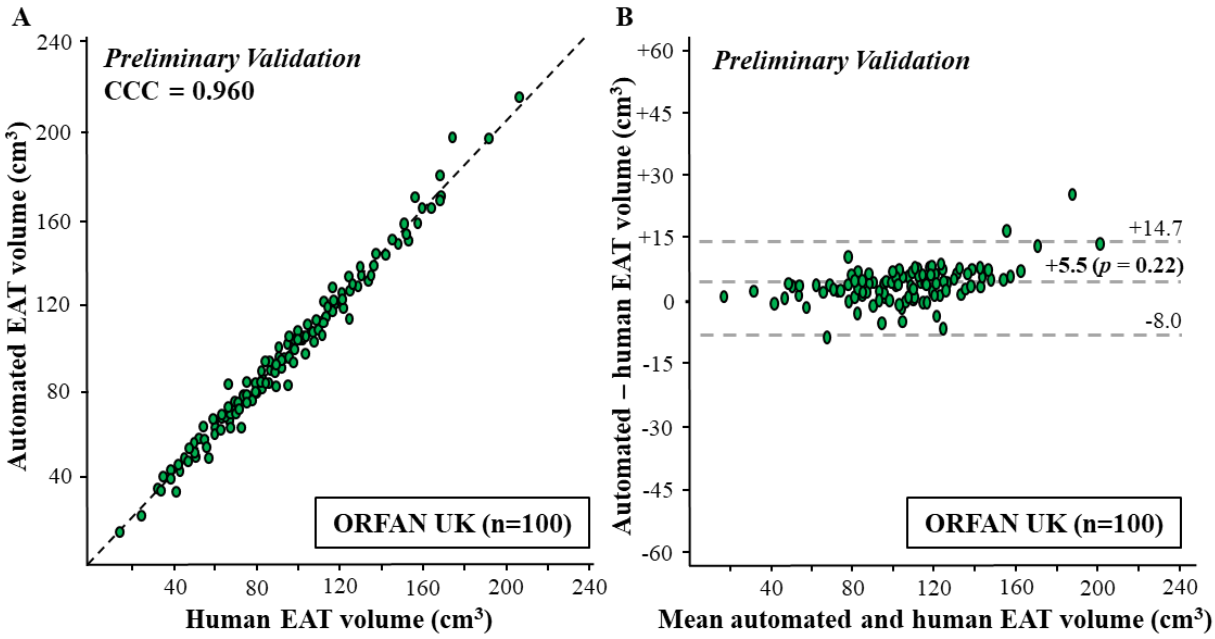

Supplementary Figure 2. Preliminary internal validation of machine learning model for whole heart segment volume assessment

Following the initial training of the model and prior to three iterations of feedback learning the model was assessed for performance against human expert segmentation in unseen CCTAs. The scatterplot (A) and Bland-Altman plot (B) demonstrate minimal variability in whole heart volume quantification between automated deep-learning machine and human expert analyst. Yellow cases indicate that the analysts indicated they assessed the individual scan to be poor quality. CCC= concordance correlation coefficient; EAT = epicardial adipose tissue; ORFAN = The Oxford Risk Factors And Non Invasive Imaging Study

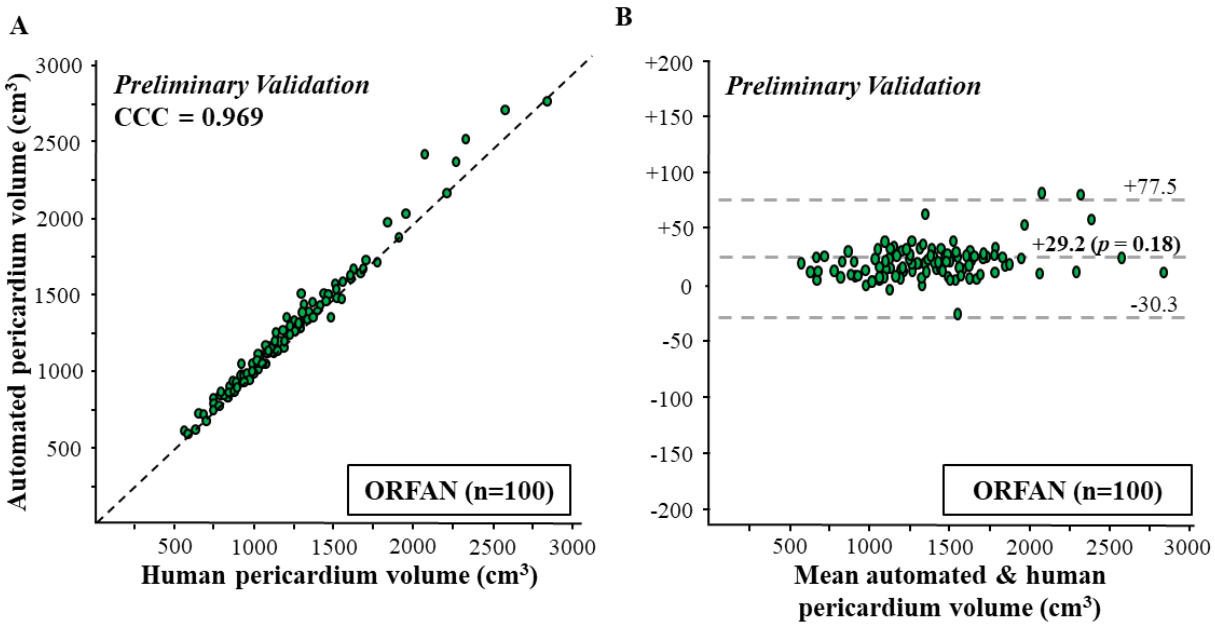

Supplementary Figure 3. Image of CaRi-Heart user work-view of manual whole heart segmentation.

The whole heart within the bounds of the visceral pericardium is manually segmented incorporating all voxels inferior to the bifurcation of the pulmonary trunk and superior to the most inferior portion of the apex of the heart. Image shows axial (red), coronal (yellow) and sagittal (green) views. Blue = segmented region.

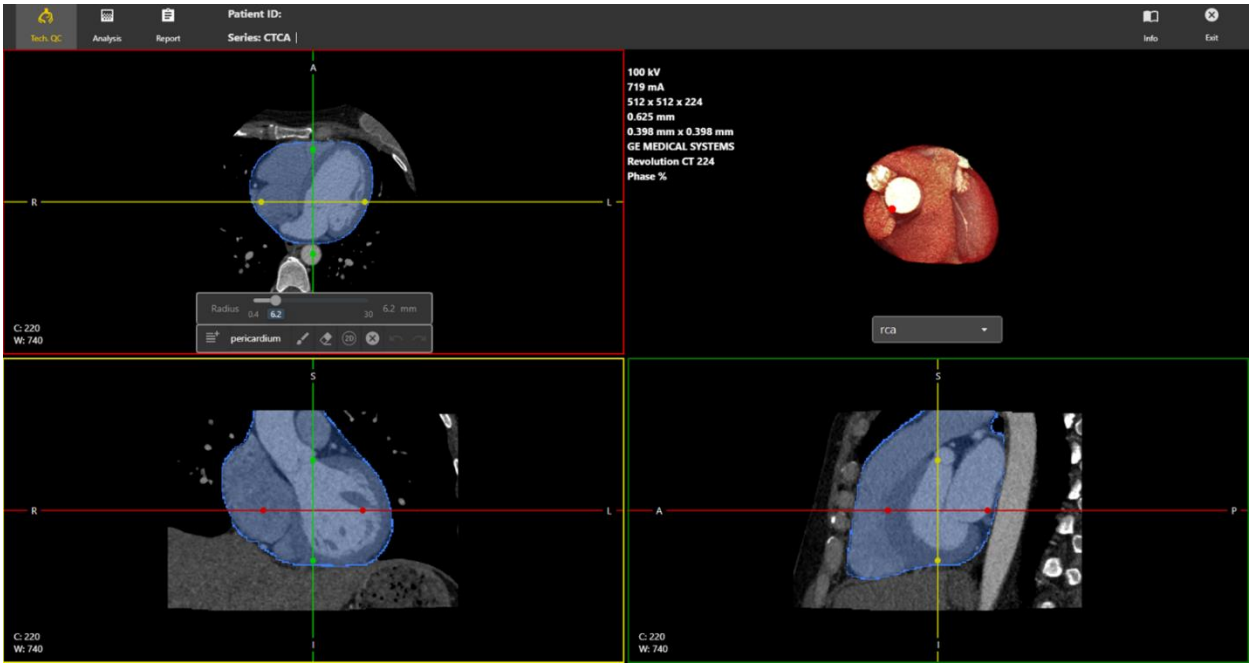

Supplementary Figure 4. Cross-sectional and longitudinal associations between EAT volume and clinical outcomes in the SCOT-HEART trial with statistically selected risk factor adjustment

Plots of cross-sectional adjusted risk models for diagnosed AF at the time of the CCTA, adjusted for age, gender, BMI, presence of hypertension, previous heart surgery, presence of valvular heart disease and presence of diabetes (A), and obstructive CAD from CCTA (any one coronary vessel with ≥50% stenosis on CCTA), adjusted for age, gender, BMI, presence of hypertension, CAC score, non-high density lipoprotein cholesterol, and active smoking (B). Odds ratio is shown per 1 standard deviation (SD) increase in EAT volume for 1558 patients randomised to receive CCTA in the SCOT-HEART trial. Plots of longitudinal hazard ratios per 1 SD increase in EAT volume in 1558 patients randomised to receive CCTA in the SCOT-HEART trial are shown for all-cause mortality (C), and non-cardiac mortality (D), both with adjustment for age, gender, BMI, presence of hypertension and diabetes, with further adjustment for active smoking in 6C. Myocardial infarction (E) is shown with adjustment for of age, gender, BMI, presence of hypertension, presence of diabetes, non-high density lipoprotein cholesterol, obstructive CAD from CCTA (any one coronary vessel with ≥50% stenosis on CCTA), and coronary artery calcium score, and stroke (F) is shown with adjustment for age, gender, BMI, presence of hypertension, presence of valvular heart disease and previous heart surgery. AF: atrial fibrillation; BMI: body mass index; CAC: coronary artery calcium score; EAT: epicardial adipose tissue; MI: myocardial infarction; Non-HDL C.: non-high density lipoprotein cholesterol.

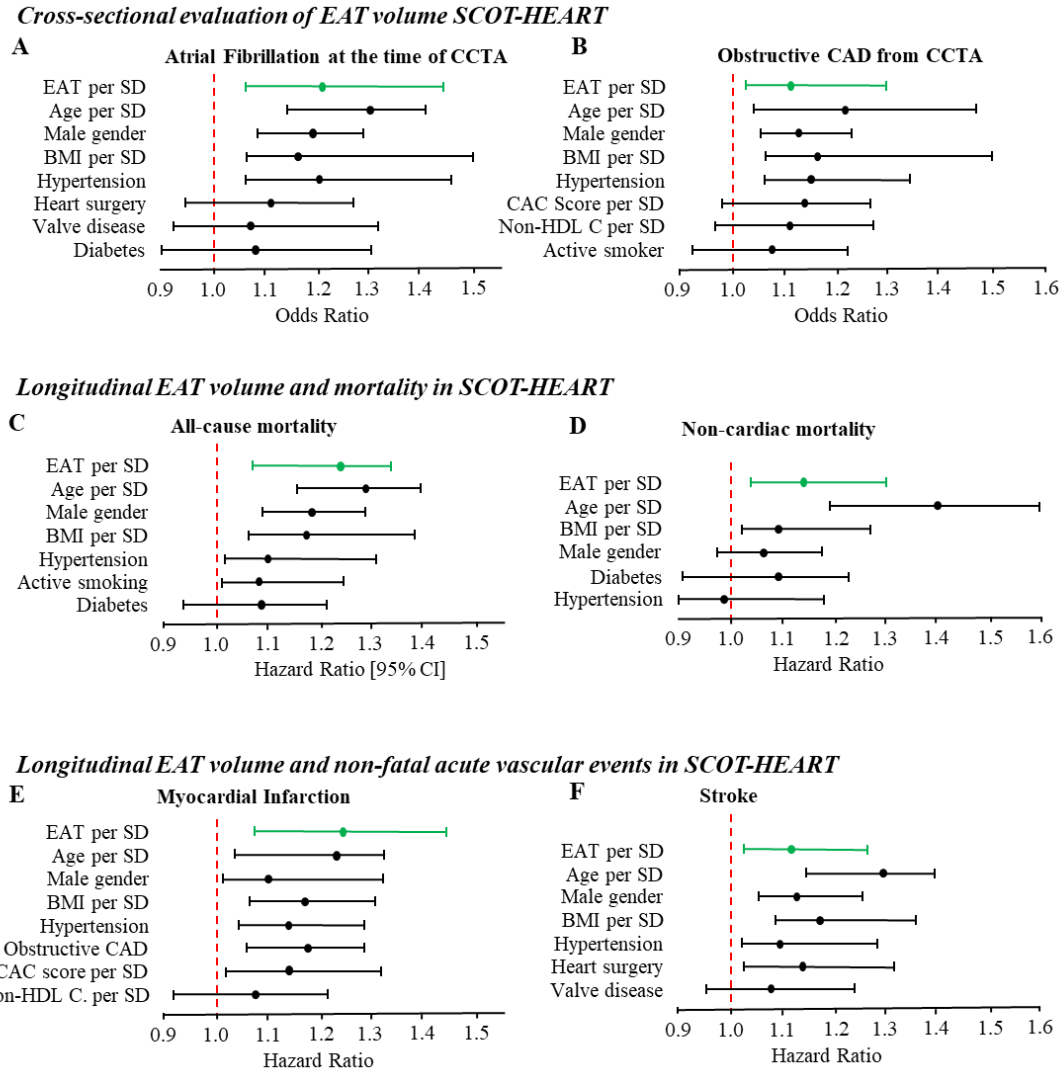

Supplementary Figure 5. EAT segmentation and whole heart volume assessment between human experts.

The scatterplot (A & C) and Bland-Altman plot (B & D) demonstrate variability in EAT segmentation (A & B) and whole heart volume segmentation (C & D) between each human analyst. CCC= concordance correlation coefficient; EAT = epicardial adipose tissue; ORFAN = The Oxford Risk Factors And Non Invasive Imaging Study

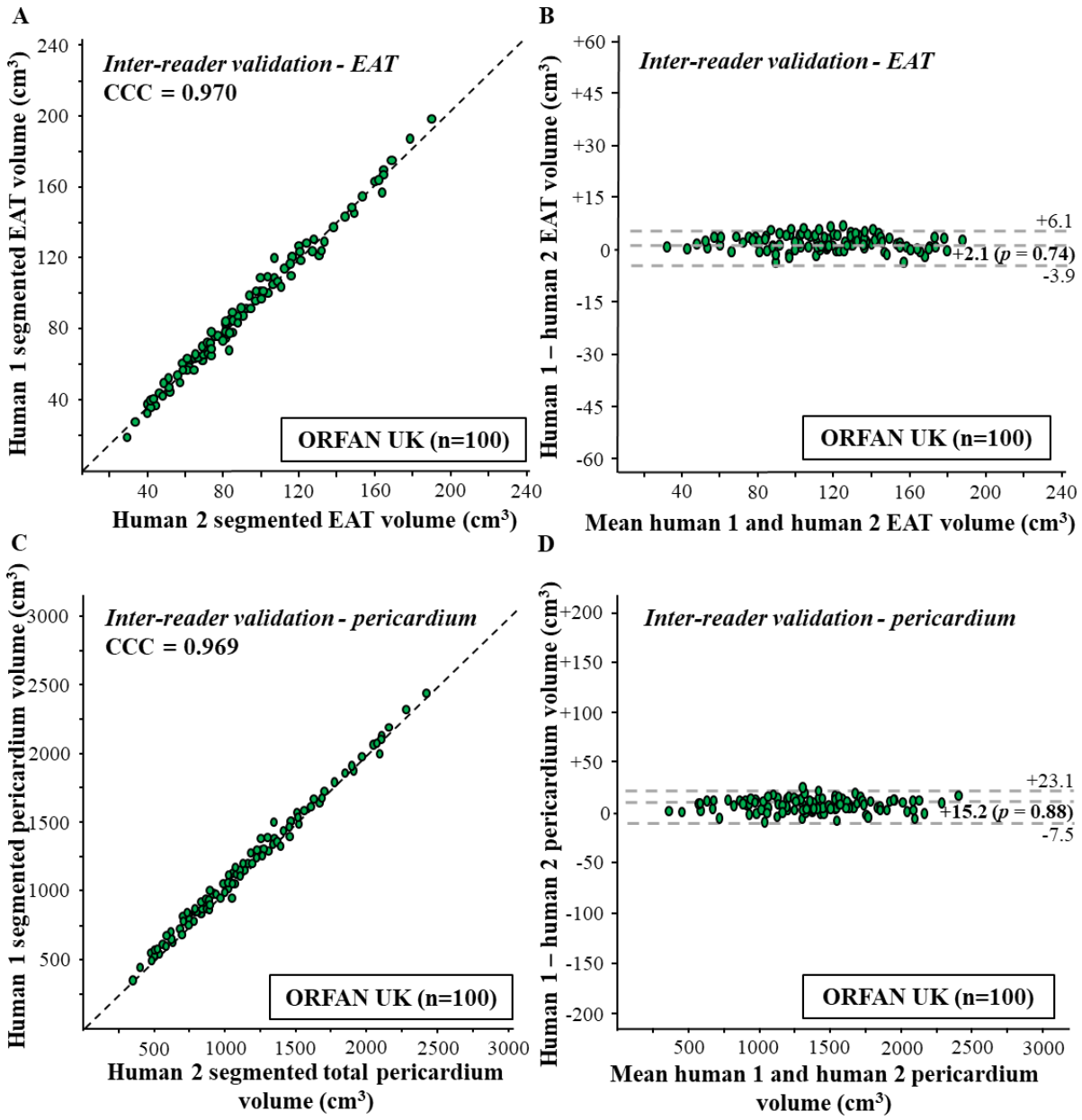

Supplementary Figure 6. Prognostic value of EAT volume for post-operative AF with adjustment for AF specific risk factors

Kaplan-Meier curve and adjusted HR for in-hospital post-operative AF (A) and long-term post-operative AF (B), with sample dichotomised by Youden's J index derived cut-point of EAT volume (high risk ≥ 198.7cm^3; low risk < 198.7cm^3), expressed per 1 SD increase of EAT volume. Adjustment is made for age, gender, previous AF diagnosis, presence of hypertension, presence of heart failure, NT-proBNP, previous myocardial infarction, BMI, and LA volume. (C,D) Time-dependent ROC curves for discrimination of in-hospital post operative AF (C) and long-term post-operative AF (D). CCTA derived LA volume (yellow) is shown alone; model 1 (red) consists of age, gender, previous AF, presence of hypertension, presence of heart failure, NT-proBNP, LA volume, previous MI, & BMI. The addition of EAT volume into model 1 is demonstrated (blue).

AF: atrial fibrillation; AUC: area under curve; BMI: body mass index; CI: confidence interval; EAT: epicardial adipose tissue;

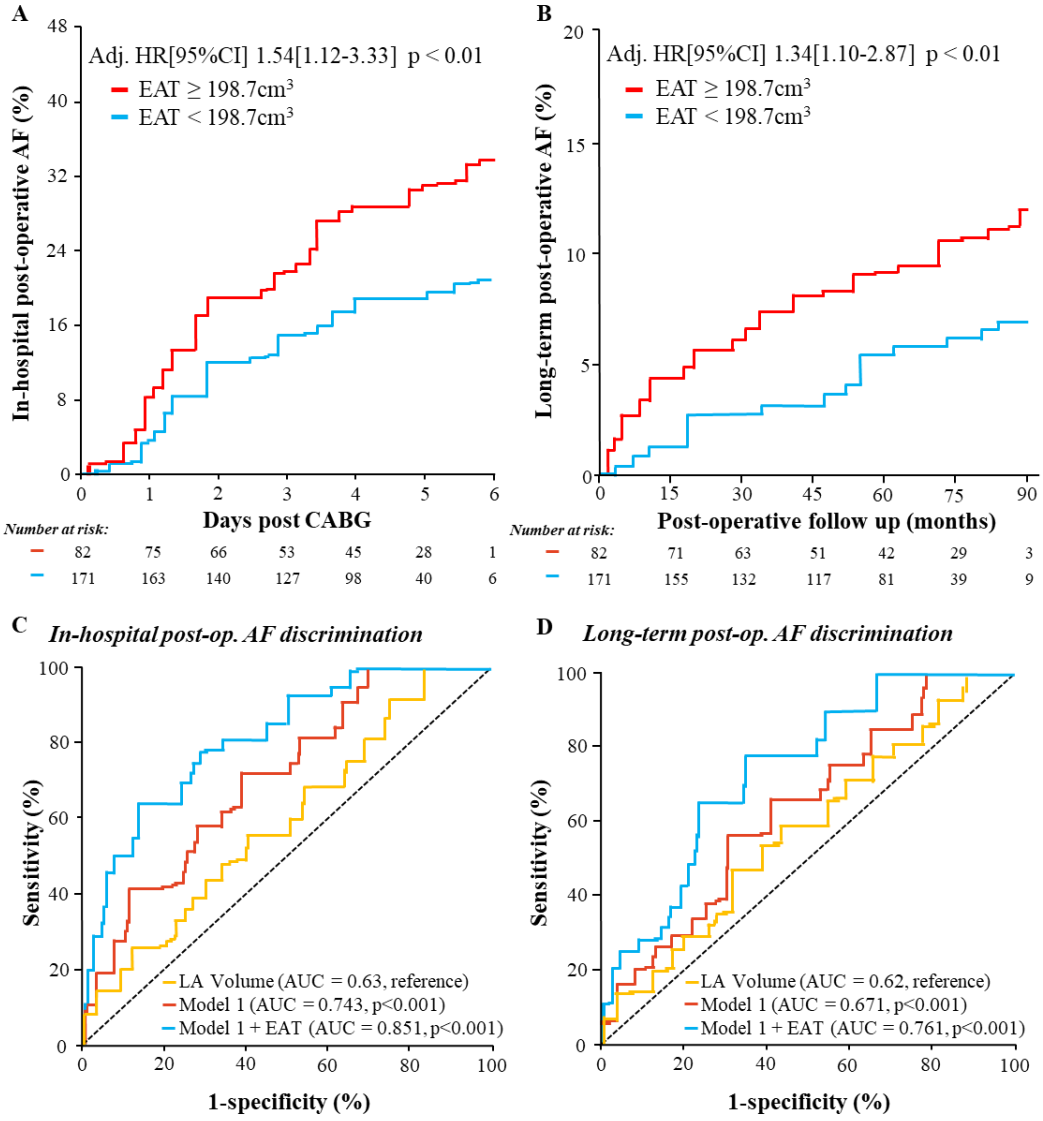

Supplementary Figure 7. Prognostic value of EAT volume for post-operative AF with adjustment for CVD risk factors including waist-hip ratio

Kaplan-Meier curve and adjusted HR for in-hospital post-operative AF (A) and long-term post-operative AF (B), with sample dichotomised by Youden's J index derived cut-point of EAT volume (high risk ≥ 198.7cm^3; low risk < 198.7cm^3), expressed per 1 SD increase of EAT volume. Adjustment is made for age, gender, hypertension, diabetes, CAC score and waist-hip ratio. (C,D) Time-dependent ROC curves for discrimination of in-hospital post operative AF (C) and long-term post-operative AF (D). CCTA derived LA volume (yellow) is shown alone; model 1 (red) consists of age, gender, hypertension, diabetes, CAC score and waist-hip ratio. The addition of EAT volume into model 1 is demonstrated (blue).

AF: atrial fibrillation; AUC: area under curve; CI: confidence interval; EAT: epicardial adipose tissue;

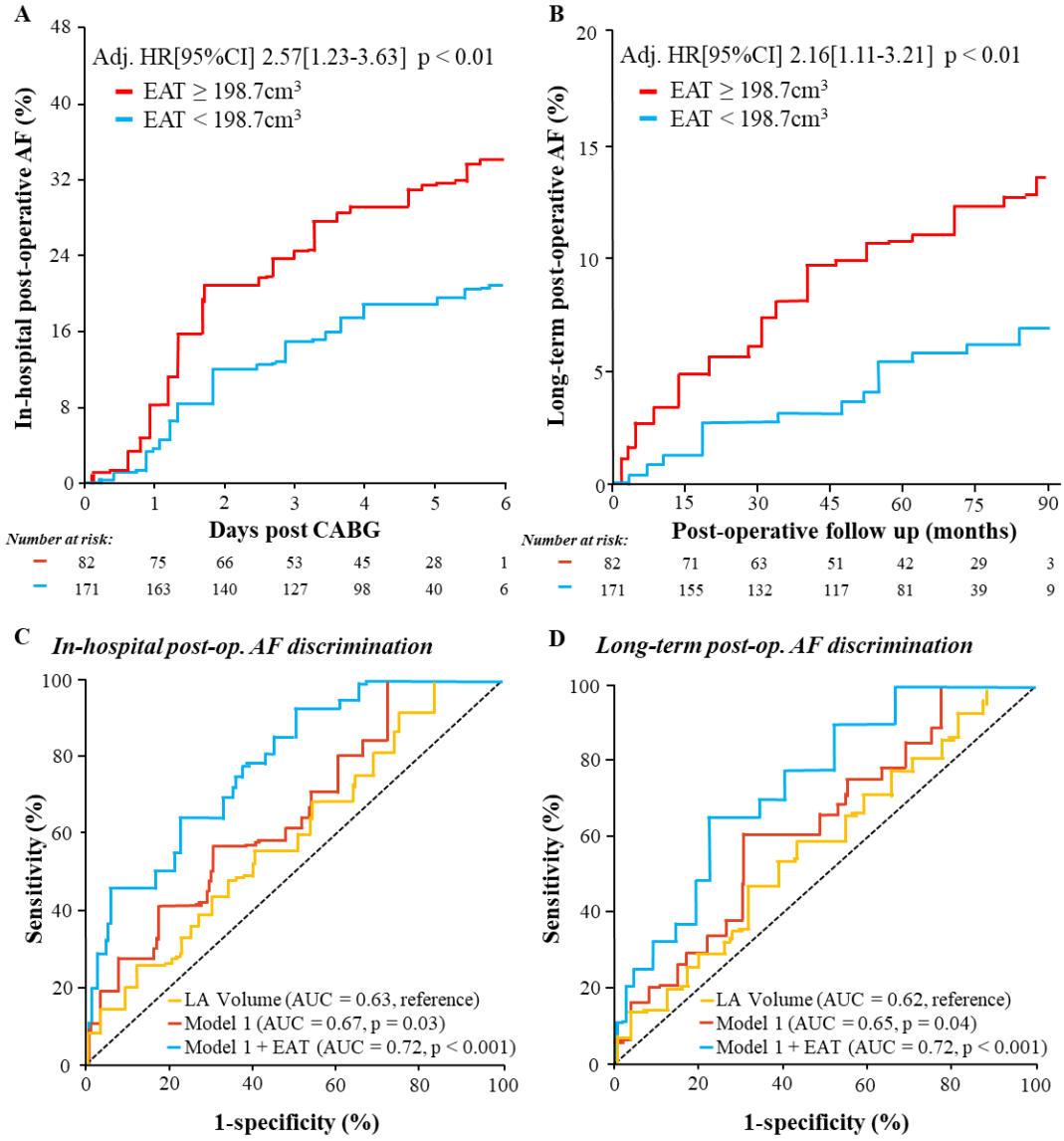

References:

1. SCOTHEART Investigators. Ct coronary angiography in patients with suspected angina due to coronary heart disease (scot-heart): An open-label, parallel-group, multicentre trial. *Lancet*. 2015;385:2383-2391
2. SCOTHEART Investigators. Coronary ct angiography and 5-year risk of myocardial infarction. *New England Journal of Medicine*. 2018;379:924-933
3. James PA, Oparil S, Carter BL, Cushman WC, Dennison-Himmelfarb C, Handler J, et al. 2014 evidence-based guideline for the management of high blood pressure in adults: Report from the panel members appointed to the eighth joint national committee (jnc 8). *JAMA*. 2014;311:507-520
4. Diagnosis and classification of diabetes mellitus. *Diabetes care*. 2014;37 Suppl 1:S81-90
5. Stone NJ, Robinson JG, Lichtenstein AH, Bairey Merz CN, Blum CB, Eckel RH, et al. 2013 acc/aha guideline on the treatment of blood cholesterol to reduce atherosclerotic cardiovascular risk in adults: A report of the american college of cardiology/american heart association task force on practice guidelines. *J Am Coll Cardiol*. 2014;63:2889-2934
6. Newby DE, Williams MC, Flapan AD, Forbes JF, Hargreaves AD, Leslie SJ, et al. Role of multidetector computed tomography in the diagnosis and management of patients attending the rapid access chest pain clinic, the scottish computed tomography of the heart (scot-heart) trial: Study protocol for randomized controlled trial. *Trials*. 2012;13:184
7. Newby DE, Adamson PD, Berry C, Boon NA, Dweck MR, Flather M, et al. Coronary ct angiography and 5-year risk of myocardial infarction. *N Engl J Med*. 2018;379:924-933
8. Thygesen K, Alpert JS, White HD, null n, null n, null n, et al. Universal definition of myocardial infarction. *Circulation*. 2007;116:2634-2653
9. Hicks KA, Tcheng JE, Bozkurt B, Chaitman BR, Cutlip DE, Farb A, et al. 2014 acc/aha key data elements and definitions for cardiovascular endpoint events in clinical trials: A report of the american college of cardiology/american heart association task force on clinical data standards (writing committee to develop cardiovascular endpoints data standards). *J Am Coll Cardiol*. 2015;66:403-469
10. Cutlip DE, Windecker S, Mehran R, Boam A, Cohen DJ, van Es GA, et al. Clinical end points in coronary stent trials: A case for standardized definitions. *Circulation*. 2007;115:2344-2351
11. Kim WH, Kim CG, Kim D-W. Optimal ct number range for adipose tissue when determining lean body mass in whole-body f-18 fdg pet/ct studies. *Nucl Med Mol Imaging*. 2012;46:294-299
12. Kvist H, Sjöström L, Tylén U. Adipose tissue volume determinations in women by computed tomography: Technical considerations. *International journal of obesity*. 1986;10:53-67
13. Mancio J, Azevedo D, Saraiva F, Azevedo AI, Pires-Morais G, Leite-Moreira A, et al. Epicardial adipose tissue volume assessed by computed tomography and coronary artery disease: A systematic review and meta-analysis. *European Heart Journal - Cardiovascular Imaging*. 2017;19:490-497
14. Oikonomou EK, Marwan M, Desai MY, Mancio J, Alashi A, Hutt Centeno E, et al. Non-invasive detection of coronary inflammation using computed tomography and prediction of residual cardiovascular risk (the crisp ct study): A post-hoc analysis of prospective outcome data. *Lancet*. 2018;392:929-939
15. Antonopoulos AS, Sanna F, Sabharwal N, Thomas S, Oikonomou EK, Herdman L, et al. Detecting human coronary inflammation by imaging perivascular fat. *Sci Transl Med.* 2017;9